Biological Effects of Osteopontin on Endothelial Progenitor Cells

Wafa Altalhi

University of Ottawa

A thesis submitted to the Faculty of Graduate Studies in partial fulfillment of the

MSc in Cellular and Molecular Medicine

23 August 2011

Cellular and Molecular Medicine – Faculty of Medicine

Dedication

To my beloved parents Audah and Eidah Altalhi, without whose help and support, nothing would have been possible.

To Ahmed for being (a good driver on call) throughout my Masters.

To my twin, Fatimah

To Abdulaziz and Safa for accompanying me in Canada

To all my sisters and brothers

Abstract

Endothelial Progenitor Cells (EPCs) are thought to participate in the healing of injured vascular endothelium by incorporating into the defect sites to mediate endothelial recovery. Recently, osteopontin (OPN) was shown to be fundamental in accelerating estrogen-dependent healing of injured blood vessels. Here, we are investigating the effect OPN has on EPC behavior. Late outgrowth human EPCs (L-EPCs) were derived from circulating monocytes isolated by leukophoresis, and grown in culture until passage six. L-EPCs were then assayed for adhesion, spreading, chemotaxis, and haptotaxis, as well as resistance to detachment by flow electric cell-substrate impedance sensing (ECIS). The results of standard and ECIS methods showed both dose and time dependent responses in cell adhesion and spreading. In addition, OPN promoted haptotactic migration of EPCs in Boyden chamber assays. L-EPCs seeded onto 10μM OPN substrates and exposed to laminar flow had grater survival and higher resistance to detachment than OPN/static and flow only conditions. CD44 and β1 integrins were only responsible for approximately 50% of L-EPCs adhesion to OPN compared to the unblocked condition. Western blots showed that Rho GTPases were activated in L-EPCs seeded on OPN. However, this activation could not be completely blocked by either CD44 or β1 integrin antagonists. These data confirm the direct effects of OPN on EPCs adhesion, and suggest that OPN works by mediating cell adhesion during vascular injury.

Key words: Endothelium, Integrins EPC, and OPN

Table of Contents

List of Figures:

Tables

List of abbreviations

BBB	Blood brain barrier
CCN	Connective tissue growth factor, Cysteine rich protein, Nephroma over expressed gene
cDNA	Complementary DNA
CD44	Hyaluronan receptor
CXCR-4	C-X-C chemokine receptor type 4, SDF-1 receptor.
E2	Estrogen
ECs	Endothelial cells
EPCs	Endothelial progenitor cells
FGF2	Fibroblast growth factor 2
FN	Fibronectin
HPC	Hematopoietic progenitor cells
HSC	Hematopoietic stem cells
iOPN	Intracellular OPN
IL-6	Interleukin-6
JAMs	Junction adhesion molecules
KDR	Kinase insert domain receptor (VEGFRII)
MAE	Murine aortic endothelial cells
MMPs	Matrix metalloproteinase
MNCs	Mononuclear cells
OPN	Osteopontin
SAH	Subarachnoid hemorrhage.
SDF-1	Stromal cell-derived factor-1
TG2	Transglutaminase-2
TN-C	tenascin C
VEGF	Vascular endothelium growth factor
vWF	Von Willebrand factor

Acknowledgments

Special thanks to my supervisor Dr. David Courtman for being an excellent guide through my Masters. Special gratitude is accorded to committee members Dr. May Griffith and Dr. Duncan Stewart for their valuable contributions to this research and for sharing their experience and perspectives. To all my friends in the three labs who are very helpful, especially to Dr. Shirley Mei for major help and advice. This research was generously supported by a scholarship from the Saudi Arabian government.

1. Introduction

Large blood vessels are composed of three main layers: 1) the tunica intima which consists of a monolayer of endothelial cells (ECs), pericytes, and the basal membrane; 2) the tunica media contains smooth muscle cells (SMCs) and an extracellular matrix (ECM) that is principally composed of proteoglycans, collagen fibers, and elastin; and, 3) the tunica adventitia is composed of the collagen-rich ECM and myofibroblasts (***Figure 1***). The focus of this project is on maintaining endothelial layer integrity (Sumpio, Riley et al. 2002; Xu 2007; Peloquin, Huynh et al. 2011).

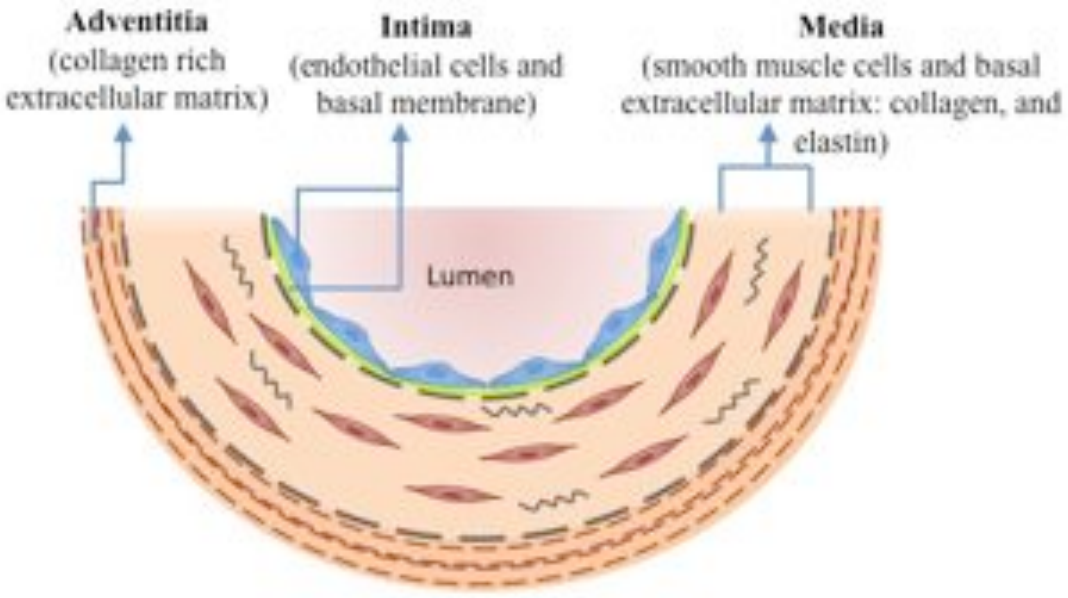

FIGURE 1: Anatomy of the large vascular wall (Peloquin, Huynh et al. 2011)

The endothelium of the tunica intima is the innermost diaphanous film of tissue that lines the luminal surface of all blood vessels. Endothelial cells (ECs) form a monolayer between the circulating blood and the vessel wall and serve critical homeostatic functions in response to various chemical and mechanical stimuli,

providing a selective barrier for macromolecular permeability. ECs can a) influence vascular remodeling via the production of growth-promoting and growth-inhibiting substances; b) modulate blood fluidity/thrombosis through the secretions of procoagulant, anticoagulant, and fibrinolytic agents; c) mediate inflammatory responses via the surface expression of chemotactic and adhesion molecules, and release of chemokines and cytokines; and d) regulate underlying vascular smooth muscle (SMC) contraction through the release of vasodilators and vasoconstrictors. Dysfunction of this EC barrier leads to pathophysiological states that contribute to the development of vascular disorders. Loss of ECs or EC dysfunction may lead to hyper-permeability to macromolecules, recruitment of leukocytes, increased production of matrix proteins, and enhancement of SMC proliferation (Sumpio, Riley et al. 2002; Peloquin, Huynh et al. 2011). This can consequently lead to serious clinical manifestations like diabetic retinopathy (Calzi, Neu et al. 2010) or atherosclerosis (Schmidt-Lucke, Rossig et al. 2005).

Exposure to injury leads ECs to produce several pro-inflammatory factors, including chemokines and cytokines such as stromal growth factor-1 (SDF-1) (Smadja, Bieche et al. 2005; Yin, Zhao et al. 2010; Kuliszewski, Kobulnik et al. 2011), adhesion molecules (L-selectin and integrins), matrix proteins (osteopontin (OPN) and thrombospondin) (Dhore, Cleutjens et al. 2001), and growth factors (vascular endothelium growth factor (VEGF; Asahara, Takahashi et al. 1999) and fibroblast growth factor (FGF-2; Chavakis, Urbich et al. 2008). Like a linked chain, each one of these factors plays a role in different steps of the healing process: cell recruitment, adhesion, proliferation, and differentiation. Activated vascular cells also increase expression of ECM proteins, which not only affect functions in the ECs, but also affect endothelial progenitor cells (EPCs), and inflammatory cells by inducing

their recruitment, migration and adhesion from the circulation to the injured area. There, they can incorporate into the vasculature in order to initiate a healing process, to restore the integrity of the endothelium (Dhore, Cleutjens et al. 2001).

Two types of ECM proteins are present in the vasculature: classical ECM and non-classical ECM proteins. Classical ECM proteins include collagen, laminin, and fibronectin. These are constitutively expressed and considered structurally important proteins that determine the physical properties of the vasculature. The non-classical ECM proteins or matricellular proteins include proteins that are involved in physiological and pathological conditions, and differ from the classical proteins in several ways. Typically expressed during specific pathological conditions, matricellular proteins are either soluble or structurally integrated into the classical ECM. Matricellular proteins can induce cell motility and migration, rather than providing a stable scaffold for cell adhesion as observed for classical ECM proteins. Matricellular proteins include osteopontin (OPN), thrombospondin-1 and 2, tenasin-C (TN-C), osteonectin and members of cystein rich protein- connective tissue factor- and nephroma expressed gene (CCN) family proteins (Arroyo and Iruela-Arispe 2010; Uede 2011).

1.1. Osteopontin (OPN)

OPN is a non-collagenous extracellular structural protein that belongs to the SIBLING glycoproteins, which were first identified in 1986 in osteoblasts. The origin of the word osteopontin is Latin: *osteo* refers to bone and *pontin* means bridge, where the name highlights OPN's capacity as a linking protein. Other names for OPN are secreted phosphoprotein 1 (SPP1), early T-lymphocyte activation (ETA-1), and bone

sialoprotein I (BSP-1) (Oldberg, Franzen et al. 1986; Nilsson, Johnston et al. 2005; Haylock and Nilsson 2006; Buback, Renkl et al. 2009).

OPN was first reported to be secreted by ECs after injury, and is now considered an essential element for estrogen (E2)/EPC-enhanced endothelial repair (Leen, Filipe et al. 2008). The role of OPN is centered on the homing and incorporation of EPCs to the site of endothelial injury. However, the mechanism by which OPN is involved in EPC-enhanced re-endothelialization has yet to be determined.

1.1.1. Expression

OPN is highly negatively charged and is composed of about 300 amino acids with a molecular weight of 33 kDa. OPN is rich in acidic residues, where 30-36% are either aspartic or glutamic acid. It is expressed by several cell types including fibroblasts, osteoblasts, macrophages, SMCs, and ECs. OPN expression is also stimulated upon exposure of cells to pro-inflammatory cytokines such as tumor necrosis factor α (TNFα), transforming growth factor β (TGFβ), interleukin-1β (IL-1β) (Yu, Fan et al. 1999), angiotensin II (Yu, Wu et al. 2000; Gauer, Hartner et al. 2003), parathyroid hormone (PTH), and estrogen (Yagisawa, Ito et al. 2001; White, Ross et al. 2005; Toutain, Filipe et al. 2009). Hyperglycemia and hypoxia are also known to increase OPN expression (Sodhi, Phadke et al. 2001; Sodhi, Phadke et al. 2001).

1.1.2. Isoforms

Full-length OPN activates a wide variety of receptors including CD44 variants and integrins (Denhardt, Giachelli et al. 2001; Scatena, Liaw et al. 2007). Its arginine-glycine-aspartate (RGD) motif that is common to many extracellular matrix proteins and known to engage many integrins has been shown to interact with αvβ1, αvβ3, αvβ5, αvβ6, and α5β1 (Courter, Cao et al. 2010 ; Barry, Ludbrook et al. 2000; Barry,

Ludbrook et al. 2000). Moreover, it can undergo post-translational modifications by phosphorylation, cleavage, or polymerization, which may be necessary for enhancing functional activity of OPN. For example, thrombin (Grassinger, Haylock et al. 2009), cathepsin D (Christensen, Schack et al. 2010), and MMP 3,5 and 12 (Gao, Agnihotri et al. 2004; Goncalves DaSilva, Liaw et al. 2010) cleaves OPN, exposing cryptic sequences such as SVVYGLR, displaying an epitope for integrin receptors of α4β1, α9β1, and α9β4 (Green, Ludbrook et al. 2001). OPN polymerization, through intra-covalent or inter-covalent linkage with fibronectin by transglutaminase, generates a bond between glutamine and lysine residues, which has been shown to increase the biological activities of OPN on mesenchymal stromal cells (Hakimzadeh, Stewart et al. 2010), human colon cancer cells, and human umbilical vein cells through binding to α3β1 integrin (Higashikawa, Eboshida et al. 2007), and also neutrophils through binding to α9β1 integrin (Nishimichi, Higashikawa et al. 2009).

1.1.3. Functions

Under normal conditions, low levels of OPN are expressed in adult cells. The level increases markedly under pathological states such as inflammation and autoimmune diseases. OPN is thought to induce recruitment and retention of macrophages and T cells to inflamed sites and it regulates the production of inflammatory cytokines in these cells (Kitamura, Iwabuchi et al. 2007; Singh, Ananthula et al. 2007). OPN is also involved in tumorigenesis and tumor metastasis, and bone mineralization and regeneration. In the cardiovascular system, OPN is expressed during atherosclerosis and valvular stenosis after myocardial infarction, as well as in regenerating endothelium at wound edges after balloon injury (Singh, Ananthula et al. 2007). OPN knockout animal models have shown normal vascular lumens, reduction in collagen, and decreased endothelium healing after injury (Myers, Harmon et al. 2003; Suzuki,

Hasegawa et al. 2010). Studies have found that OPN induces adhesion and migration of numerous cell types, including ECs, SMCs, and osteoclasts (Liaw, Almeida et al. 1994; Dai, Peng et al. 2009). In addition to inhibiting apoptosis in ECs, OPN is also involved in angiogenesis and post-ischemic neovascularization (Pagano and Haurani 2006; Zhao, Johnson et al. 2007; Duvall, Weiss et al. 2008). Together with VEGF, OPN has been found at the wound edges of regenerating endothelium (Senger, Ledbetter et al. 1996; Infanger, Shakibaei et al. 2005), which suggests that OPN mediates acceleration of re-endothelialization and endothelial repair (Liaw, Lindner et al. 1995). However, a recent report showed that *in vitro*, OPN overexpression dramatically impairs re-endothelialization by inhibiting EC motility and promoting strong adhesion (Leali, Moroni et al. 2007). Interestingly, OPN was shown to be critical in estrogen-enhanced re-endothelialization through promoting bone marrow progenitor cells' homing adhesion to the site of injury (Leen, Filipe et al. 2008; Molin, van den Akker et al. 2008). Thus, OPN's effect on endothelial regeneration and repair need to be clarified.

1.2. Endothelial Progenitor Cells (EPC)

Asahara was the first to describe EPCs in 1997 as CD34-expressing circulating progenitor cells that show clonal potential, stemness characteristics, adherence to matrix molecules and the capacity to differentiate into the endothelial cell phenotype *in vitro* (Asahara, Masuda et al. 1999). Asahara, as well as others, found evidence that EPCs may contribute to neoangiogenesis within adult mice and rabbits, in which CD34- and Sca-1-enriched mononuclear cells promoted new blood vessel formation in injured areas, enhanced perfusion, and lead to recovery of ischemic tissue (Asahara, Takahashi et al. 1999; Kalka, Masuda et al. 2000; Kalka, Masuda et al.

2000; Masuda, Kalka et al. 2000). The discovery of EPCs initiated the hypothesis that these cells have a role in postnatal endothelial biology. Now, it is believed that both mature ECs and EPCs contribute to the regeneration of the endothelium (Masuda, Kalka et al. 2000). Past research has made serious attempts to optimally define EPCs. Generally, two approaches are applied to identify EPCs: a) the identification of cells markers; and, b) the assumption of the presence of endothelial precursors via the identification of cells bearing mature endothelium characteristics.

1.2.1. Isolation

Studies have identified two distinct populations of EPCs isolated from bone marrow and blood. These two populations were named according to their culture days *in vitro*: early-EPCs appear in culture at day 7 and, late outgrowth EPCs, which emerge between 2 and 3 weeks after original seeding. Although both EPC types share common features including the expression of CD34, KDR, lectin binding, and LDL uptake, EPCs types have distinct characteristics with respect to in vitro morphology, cell surface markers, and function ***(Table,1)*** (Mead, Prater et al. 2008) **.**

TABLE 1: GENERAL COMPARISON BETWEEN EARLY AND LATE EPCS

		Early EPCs Circulating angiogenic cells	Late EPCs Colony forming cells
		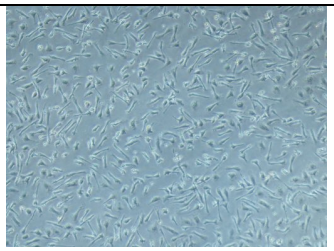	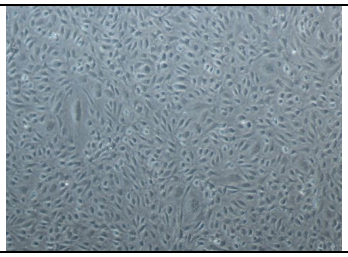
Morphology		Spindle-like with one spherical side	Flat, cobblestoned
Proliferation		Low	High
Markers	Positive	CD133,31,14,45,115,34, KDR, and Ac-LDL	CD 34,31,144,105,146,KDR, Ac-LDL, and vWF
	Negative	CD144	CD14,45,115, and 133
Contribution toward vessels formation and re-endothelialization		Paracrine effect (secrete angiogenic factors)	Contribute to injured endothelium and new vessels

Early-EPCs were identified as being spindle-shaped cells that are rounded at one end and they express CD34, CD133, vascular growth factor receptor 2 (Flk-1/KDR), CXCR4, and CD105. However, this type of cell does not proliferate, and is not capable of forming net like structures *in vitro*. They are also thought to support angiogenesis through a paracrine effect, which led to designating them the name such as circulating angiogenic cells. On the other hand, late-EPCs are identified as endothelial colony-forming cells that show endothelial lineage markers, e.g. von Willibrand Factor (vWF), vascular endothelial cadherin, CD146, KDR, vascular growth factor, but no hematopoietic surface markers (CD45 and CD133). In contrast to early EPCs, late EPCs have the capacity to form intact networks *in vitro*. Therefore, late-EPCs are a promising therapeutic option for re-endothelialization, not only because of their capability for self-renewal and differentiation into an EC-lineage, but also due to their morphology, markers, functional protein expression, growth

characteristics, and vascular network formation *in vitro*, which better resemble ECs than early-EPCs (Hur, Yoon et al. 2004; Prater, Case et al. 2007; Yoder, Mead et al. 2007; Mead, Prater et al. 2008; Timmermans, Plum et al. 2009; Steinmetz, Nickenig et al. 2010).

1.2.2. EPCs in Cardiovascular Diseases

After 14 years of extensive research of EPC biology, there is no definitive answer regarding how EPCs function. Focusing on factors and conditions that affect mobilization and homing, as well as their roles in neovascularization and re-endothelialization, researchers have been able to present data confirming that EPCs are strongly related to cardiovascular pathophysiology (Kirton and Xu 2010). Even though the factors leading to the mobilization of EPCs from bone marrow and homing to the site of injury have not been fully explored, defects in EPC mobilization and function have been shown to correlate with cardiovascular risks factors ***(Figure 2)*** (Kirton and Xu 2010; Steinmetz, Nickenig et al. 2010).

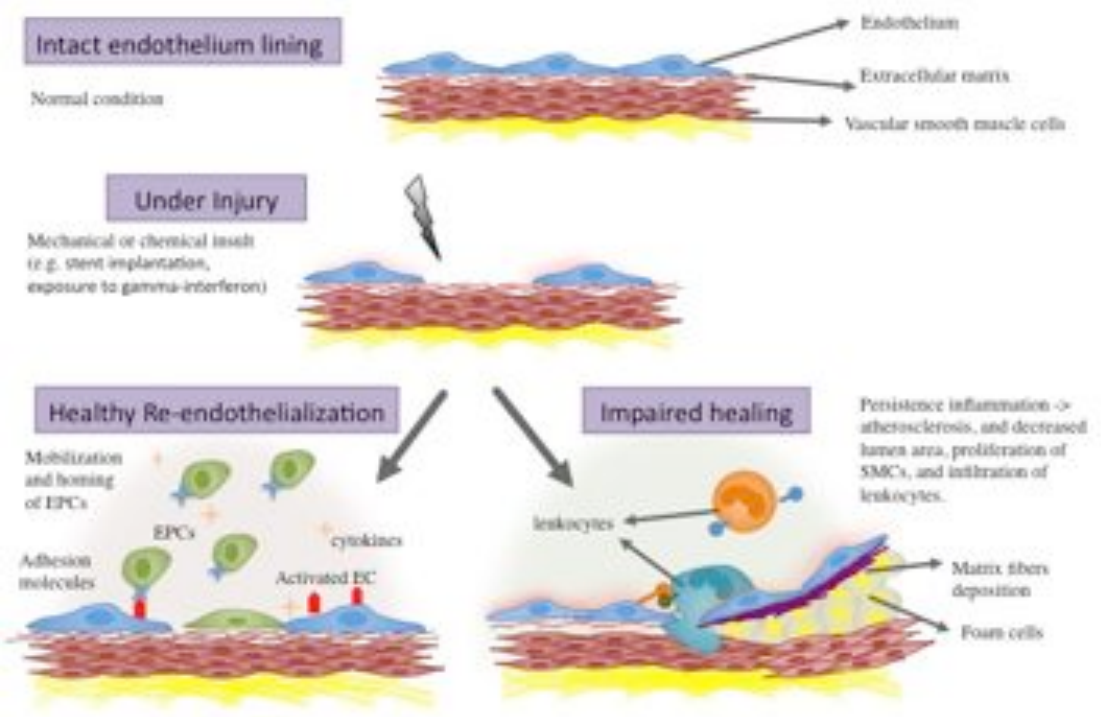

FIGURE 2: Role of EPCs in maintaining endothelium integrity during normal and abnormal states. When exposed to an injury stimulus, ECs secrete cytokines and express adhesion molecules to which EPCs bind and home to the site of injury. EPCs in turn start to gain a more mature endothelium phenotype and fill up the injured space. This function of EPCs in maintaining the integrity of the vascular endothelium layer is impaired in patients with cardiovascular risk factors such as hyperglycemia, which reduces the number and the functional activity of circulating EPCs after injury. Thereby, endothelium healing is delayed and eventually increases infiltration of leukocytes, lipid accumulation in sub-endothelium compartments of the vasculature, and induces SMC proliferation, which will reduce the luminal area and establish atherosclerosis.

1.2.3. Mobilization and Homing of EPCs

To determine the mechanism by which EPCs are released from bone marrow into the blood, researchers have studied the response to cytokine stimulation as well as the relationships to cardiovascular conditions. It was observed that the number of EPCs is boosted in cases of acute ischemia (Takahashi, Kalka et al. 1999), myocardial infarction (Huang, Hou et al. 2007), unstable angina (Leone, Valgimigli et al. 2009), or after coronary artery intervention (stent implantation) (Padfield, Newby et al. 2010). Moreover, there is an inversely related correlation of EPC number and function to cardiovascular risk factors (Schmidt-Lucke, Belgore et al. 2005), such as

hypertension and diabetes (Smadja, Gaussem et al. 2009; Smadja, Mauge et al. 2010; Smadja, Mauge et al. 2011), and diabetes alone (Calzi, Neu et al. 2010), in addition to conditions such as acute myocardial infarction (Schmidt-Lucke, Rossig et al. 2005), increasing age, and renal disease (Werner, Kosiol et al. 2005; Werner, Wassmann et al. 2006; Calzi, Neu et al. 2010; Ueno H and Inaba M 2011).

By examining the underlying mechanisms, studies have reported that there are a number of cytokines responsible for the induction of EPC mobilization. These include: SDF-1 (Lin, Chen et al. 2009; Yin, Zhao et al. 2010; Kuliszewski, Kobulnik et al. 2011) and VEGF (Asahara, Takahashi et al. 1999; Schmidt-Lucke, Belgore et al. 2005), which are produced in ischemic areas (Takahashi, Kalka et al. 1999); GM-CSF, which is a proinflammatory cytokine that promotes circulation of leukocytes; and the production of erythropoietin, estrogen (Krasinski, Spyridopoulos et al. 1997; Masuda, Kalka et al. 2007; Leone, Valgimigli et al. 2009), and prostaglandin (Kawabe, Yuhki et al. 2011). Interestingly, most of these factors work though the activation of nitric oxide (Murohara, Asahara et al. 1998; Toutain, Filipe et al. 2009)

The recruitment of circulating progenitor cells to the endothelial monolayer of the peripheral vasculature (typically where angiogenic events are occurring) is defined as “homing”. Studies have reported a few adhesion molecules that support EPC homing, such as JAM-A, which induces CD34+ve EPCs to bind to ECs after injury; and αvβ3(Chavakis and Dimmeler 2011); cell adhesion is enhanced by the chemokine SDF-1 which binds to CXCR4 expressed in ischemic regions (Smadja, Bieche et al. 2005; Shepherd, Capoccia et al. 2006; Yin, Zhao et al. 2010). Recently, OPN was reported to be crucial for the homing response of bone marrow-derived progenitor cells, which includes EPCs, to the site of vascular injury. This was confirmed when the number of circulating mononuclear cells (MNCs) was increased after estrogen

stimulation, accompanied by delayed endothelial repair in OPN knockout mice (Xu 2007; Chavakis, Urbich et al. 2008; Leen, Filipe et al. 2008; Chavakis and Dimmeler 2011).

1.2.4. Re-Endothelialization

EPCs have been shown to promote tissue neovascularization through their angiogenic activity (Asahara, Takahashi et al. 1999; Hu, Davison et al. 2003; Shepherd, Capoccia et al. 2006; Smadja, Bieche et al. 2008; Smadja, Mauge et al. 2009). EPCs are considered to have a key role in the maintenance of vascular integrity and to act as ‘‘repair’’ cells in response to endothelial injury to avoid atherosclerosis (Hibbert, Olsen et al. 2003; Xu 2007; Lin, Chen et al. 2009). The participation of EPCs in re-endothelialization of injured vasculature is still under extensive investigation. The Itoh group have attempted to frame the functions of different EPC subtypes in vascular healing theoretically. They contend that early-EPCs start the process by homing to the site of injury, where they support endothelial healing by secreting cytokines, and temporarily incorporating into the vasculature as place holders for L-EPCs. L-EPCs then permanently incorporate and differentiate into fully mature endothelial cells (Xu 2007; Yamahara and Itoh 2009). Interestingly, re-endothelialization and reduced neointimal thickening of the injured vasculature was also reported to occur in part by tissue resident L-EPCs rather than bone marrow L-EPCs (Timmermans, Plum et al. 2009; Wang, Lin et al. 2009; Liu, Li et al. 2011).

1.3. OPN and EPCs:

Adverse vascular remodeling is a significant clinical consequence of advanced atherosclerosis. Limiting the development of this process is dependent upon the timely re-endothelialization of the neointimal surface with a functional endothelial monolayer. Many studies have found evidence that EPCs play a crucial role in

vascular regeneration and re-endothelialization. These studies showed that EPCs are mobilized to the peripheral blood circulation in response to an injury stimulus, where they will either release factors to mediate the healing process or differentiate into a more mature endothelium lineage and incorporate into the vasculature (Xu 2007; Wang, Lin et al. 2009; Yin, Zhao et al. 2010; Liu, Li et al. 2011).

EPCs target the injured site and stimulate re-endothelialization. Mobilization and homing, as well as the initiation of the re-endothelialization by EPCs involve the synergistic effects of a number of variables that include the response to growth factors and cytokines secreted at the site of injury. These factors may include VEGF, β-FGF, SDF-1, and estrogen (E2).

Leen et al. (2008) showed that OPN is an essential element for estrogen (E2)-enhanced endothelial repair. This study indicated that the number of bone marrow-derived cells mobilized into the blood stream was not affected in wild-type mice (OPN+/+) or OPN-deficient mice (OPN-/-). However, endothelial repair was lost in OPN-/-. This study not only showed OPN expression in the wound periphery of an injured artery in wild-type mice compared to uninjured vessels, it also indicated increased endothelial repair and MNC incorporation into the wounded area with OPN overexpression. These data suggested that OPN works by mediating cell adhesion to wound areas (Leen, Filipe et al. 2008; Molin, van den Akker et al. 2008).

OPN has been shown to stimulate cellular adhesion, migration, and survival. Indeed, OPN was identified as a chemotactic agent that contributes to leukocyte recruitment to the site of inflammation and facilitates cell adhesion to wound areas. In addition, it was also recognized as a powerful anti-apoptotic factor in many conditions. For example, in cancer cells, OPN acts by blocking apoptosis after cellular detachment from the surroundings (Courter, Cao et al. 2010 ; Denhardt, Giachelli et

al. 2001; Infanger, Shakibaei et al. 2005; Duvall, Weiss et al. 2008; Leen, Filipe et al. 2008; Dai, Peng et al. 2009).

Suzuki *et al.* showed a beneficial effect of OPN on the recovery of blood brain barrier (BBB) disruptions (Suzuki, Hasegawa et al. 2010). They noticed that after subarachnoid hemorrhage (SAH), OPN expression was 2 folds increased in astrocytes and capillary ECs after subarachnoid hemorrhage (SAH) compared to normal condition $p< 0.05$. In contrast to the normal condition, the disrupted BBB was exacerbated when endogenous OPN was blocked, whereas recombinant OPN treatment of mice restored the recovery process. OPN is also notable for contributing to normal cardiovascular physiology. Myers *et al.* tested the critical physiological effects of OPN on the cardiovascular system (Myers, Harmon et al. 2003). They reported that compared to wild-type mice, OPN-null mice showed increased heart rate and lower blood pressure in normal conditions. In addition to significant differences shown in the remodeling response after carotid artery ligation, there was a 10-fold decrease in leukocyte adhesion and invasion. They also observed that although OPN-null mice had smaller neointimal lesions than wild-type mice, they had more constrictive remodeling, which resulted in similar lumen areas. In conclusion, the researchers were able to confirm the ability of endogenous OPN in maintaining normal vascular physiology, and in regulating the remodeling response by contributing to vascular compliance and the inflammatory response.

Similarly, Nilsson *et al.* found that OPN is a key regulator for normal physiology of the hematopoietic stem cell (HSC) niche (Nilsson, Johnston et al. 2005). OPN is responsible for keeping HSCs quiescent in endosteal bone surfaces. OPN can induce primitive hematopoietic cell adhesion via β1 integrins and

suppression of proliferation of primitive hematopoietic progenitor cells (HPCs) *in vitro*.

OPN contributes to endothelial regenerative capacity. Liaw *et al.* reported that OPN mRNA levels increased in the wound edges of arterial endothelium after balloon catheter denudation compared to that observed in an uninjured rat (Liaw, Almeida et al. 1994). This increase declined after regeneration was complete. In addition, they showed that recombinant OPN stimulated cell adhesion and directed migration through the αvß3 receptor. Similarly, Duvall *et al.* provided evidence for a role for OPN during ischemic limb revascularization *in vivo* (Duvall, Weiss et al. 2008). In their experiment, they investigated the role of OPN in recovery from hind-limb ischemia in wild type and OPN–/– mice. They reported that OPN–/– mice had a significant recovery delay of ischemic foot perfusion, impaired collateral vessel formation, and significantly decreased functional capacity of the ischemic limb. In addition, a significant reduction of monocytes/macrophages in OPN–/– mice in response to chemo-attraction by monocyte chemotactic protein-1 (MCP-1) was observed. These data present evidence that OPN is a regulator of *in vivo* postnatal vascular growth.

Recently, Vaughan *et al.* investigated the role of OPN downregulation in EPCs with a decreased angiogenic response in type-1 diabetes mellitus (Vaughan, Duffy et al. 2009). They reported that EPCs from OPN knockout mice showed a significantly lower number of tubules compared to wild-type mice. This reduction was reversed when the cells were pre-incubated with recombinant OPN. Interestingly, they also found that conditioned media from wild-type cells and recombinant OPN pre-incubated knockout EPCs were able to induce EPC tubule formation. Both cellular conditions were found to express interleukin-6 (IL-6) and fibroblast growth

factor (FGF) at a higher level than OPN knockout EPCs. Taken together, their data suggested that OPN enhances EPC angiogenic function via an autocrine mechanism in which OPN is secreted first, and then induces the expression of a variety of angiogenic proteins.

Leali *et al.* reported that in murine aortic endothelial cells, intracellular OPN (iOPN) is essential for vascular endothelial cell adhesion (Leali, Moroni et al. 2007). When transfected with OPN cDNA, these cells had both strong adhesion and spreading to immobilized OPN. In addition, iOPN reduced murine endothelial cell motility in the Boyden chamber assay, and reduced their ability to repair a wounded monolayer. This likely occurred by inhibiting cell migration via α_v integrin engagement by the extracellular matrix-immobilized protein. Therefore, their data suggests that OPN can in some situations inhibit cell motility through induction of strong adhesion.

OPN is also a promising coating for biomaterial implants. It has been shown to be a particularly strong mediator of cell attachment and spreading when coated on hydrophilic surfaces and these surfaces may be most relevant to cardiovascular biomaterials (Malmstrom, Christensen et al. 2010). It is also thought to decrease foreign body reaction when used to coat implanted biomaterials (Liu, Chen et al. 2008). Liu *et al.*tested this hypothesis by coating OPN on a surface polymer (HEMA-*co*-AEMA). The material was then implanted subcutaneously for 7 or 28 days in wild-type mice. Cells showed more adhesion and spreading and reduced capsule formation in the coated implant compared to the uncoated polymer implant. These data demonstrate that OPN coating of putative biomaterials may help improve biocompatibility after implantation (Liu, Chen et al. 2008).

In summary, EPCs have been shown to be involved in the repair and re-endothelialization of injured vasculature. OPN was reported to be secreted by ECs after injury, and is considered an essential element for Estrogen (E2)/EPC-enhanced endothelial repair. The role of OPN is centered on the homing and incorporation of EPCs to the site of endothelial injury. However, the mechanism by which OPN is involved in EPC-enhanced re-endothelialization has yet to be determined. The purpose of this project therefore is to determine the effects of OPN on EPCs. We hypothesize that **OPN acts as an adhesion as well as a chemotactic agent for L-EPCs.** The objectives are ***(1)*** To determine the functional effects of OPN on L-EPCs. ***(2)*** To determine the signaling pathway by which OPN induces these effects.

2. Materials and Methods

2.1. Cell culture:

Cells were obtained from leukophoresis products harvested from healthy human subjects. The products were processed in multi-step procedures; starting by Ficoll density gradient separation of mononuclear cells, followed by seeding onto fibronectin for 2-3 weeks during which L-EPCs emerge from the cell culture. They are then frozen after the third passage. Cell isolation and freezing were performed previous to initiation of this project by other lab members. Upon receiving, cells were thawed and seeded in flasks coated with 1 μg fibronectin (Roche, USA) in 1 ml of phosphate buffer saline (PBS) (BioWhittaker, Lonza, USA) and fed with Endothelial Basal Medium-2 (EBM-2) (Clonetics, Lonza, USA) supplemented with endothelial growth supplements (singleQuots, Loza, USA) and 20% human serum (Lonza, USA). The next day, media was changed after washing the cells with PBS to remove any remaining dimethyl sulfoxide (DMSO) (Fisher scientific, USA). Then, the media was changed every third day until confluent. For expansion, cells were washed with PBS and detached using a non-animal origin cell dissociation enzyme TrypLE^{TM} (GIBCO, USA). Cells were then washed and re-plated on the 1 μg/ ml fibronectin PBS-coated flask (Corning, USA), with media changes every third day. To freeze cells, they were detached with TrypLE^{TM}, neutralized with complete media, and then washed three times with PBS. Cells from each T75 flask were suspended in 1 ml of freshly prepared 10% DMSO cryopreservation media (10% DMSO in 10% serum EBM-2 and endothelial growth supplements). The cells were then frozen overnight at -80°C, and then moved the next day to liquid nitrogen and stored until use. To monitor the

ideal growth of the cells, images of the cells were taken after each process i.e. thawing and expansion.

2.2. Protein coating:

For this *in vitro* study of L-EPC adhesion to OPN, we immobilized OPN on different surfaces. Protein coatings for OPN (R&D, USA) and fibronectin were prepared in PBS (when plates or migration membranes were used), or in 0.1 M NaOH (when cell substrate impedance sensing special slides were used, according to manufacturer's instructions). Coatings were freshly prepared by incubating surfaces in solutions overnight at 4°C followed by 1 h at 37°C. Prior to use nonspecific binding was inhibited by incubating wells with 10% bovine serum albumin (BSA) (Cell Signaling, USA) for another 1 h at 37°C. Wells were then washed and filled with PBS until use.

2.3. Adhesion Assay:

2.3.1. Cell counts (Crystal Violet staining)

This assay was applied to determine if OPN induces L-EPC adhesion. For this purpose, both adherent and spreading EPCs are calculated over serial concentrations of OPN. Here, we evaluated the effects by standard quantitative adhesion and spreading assays. The experiment started by coating 24-well plates (Corning, USA) with serial concentrations of OPN 0, 1, 10, 100 μM in PBS as indicated above. The confluent L-EPCs were incubated in serum-reduced media (2% serum media) for 1 day, L-EPCs were then detached using TrypLE™ and washed with PBS. After that, 500 μl of 5×10^3 cells/ml in basal media with 2% serum were added to the coated wells and incubated at 37°C for 4 h. At the end of the incubation, media was removed by inverting the plate onto an absorbent pad. The wells were washed three times with

PBS, and then fixed with 4% paraformaldehyde for 10 min at room temperature. The fixative solution was then removed and wells were washed three times with cold PBS. In order to visualize the cells, the wells were incubated with 0.5% Crystal Violet for 30 min at room temperature. The wells were then washed three times with ddH_2O and allowed to dry overnight. Adherent cells were counted using phase contrast microscopy (NIKON Eclipse, T5100) at 20X in 4 fields, and number of adherent cells was averaged per each well. For spreading, cell area was calculated with microscope-attached software (Digital sight DS-L2 control unit) at 40X. Then, cells with area more than 1500 μm^2 were counted in 4 fields per well under 40X, and then a percentage was calculated for the total cells count per each well.

2.3.2. Automated real time electric cell-substrate impedance sensing (ECIS)

This assay was applied to compare the adhesion of L-EPCs to OPN with FN and uncoated surface. As in the manual quantitative adhesion assay, we hypothesized that L-EPCs adhere to OPN and that this adhesion can induce cell survival after 20 h. For this reason the ECIS instrument (Applied Biophysics, USA) was used. This instrument electrically monitors cell behavior, including adhesion and spreading, in tissue culture by measuring the impedance across small gold film electrodes produced by the adherent cells. The electrical signals are generated through the electrolyte rich media and move freely when no cells are covering the electrodes. However in the presence of cells, these electrical waves encounter cell membranes, which act as an insulator and produce resistance. The assay employed was similar to that developed by Rotundo, TM et al. (2002) for endothelial cells attached to fibronectin coatings. The wells of ECIS chamber slides were coated with 10 μM of OPN or FN in 0.1 M NaCl overnight at 4ºC, or kept uncoated as indicated in Section 2.2. The next day,

coating solutions were removed and wells were blocked with 10% BSA for 1 h at 37ºC. Then, the slides were inserted into the monitoring station and connected to the ECIS machine (8W10E, Applied Biophysics, USA). Readings commenced by calibrating capacitance with 400 µl of media to 50 nanofarads. The chambers were removed from the station and media was substituted with 400 µl of 5 $\times 10^3$ cells/1 ml media. The cell suspension was taken from confluent cells that were incubated in serum-reduced media (2% serum media) and were detached using TrypLE™, then washed with PBS. The assay lasted for 20 h at 37ºC.

2.4. Migration Assay:

To detect the haptotactic activity of OPN, the polyethylene terephthalate (PET) membrane inner surface of 24-well inserts (BD Falcon, USA) was coated with 50 µl of 1 µg/ml OPN as indicated in Section 2.2. To detect the chemotactic activity, inserts were kept uncoated while OPN was supplemented to the lower compartment with the serum-reduced media (2% serum media), see ***Figure 3***. A confluent layer of L-EPCs was incubated in 2% serum media one day before the assay. Next day, media was removed and cells were washed with PBS three times then detached using TrypLE™. After 10 min, TrypLE™ was neutralized with 20% serum complete media and cell suspensions were centrifuged at 220×g for 5 min. Then, supernatant was removed and cells re-suspended in 5 ml of PBS and re-centrifuged at 220×g for 5 min. After that, 250 µl of 3×10^5 cells/ml in 2% serum media were added to the upper compartment and 750 µl of 2% serum media were added into the lower compartment of the inserts. Cells were incubated at 37°C for 16 h. At the end of the incubation, media in the upper compartment was removed and the inserts removed gently and washed three times with PBS. Non-migrating cell were removed with PBS soaked cotton swabs and then migrating cells were fixed with 4% paraformaldehyde for 10 min at room

temperature. The fixative solution was removed followed by 3 times washing with cold PBS. To detect migration, the nuclei of migrating cells were stained with DAPI at 1:4000 ratios in PBS for 5 min and then washed for another 3-times in PBS. Membranes were then cut out of the inserts with a sharp blade and mounted with Mowiol medium. After that, migrated cells were detected by counting cells per area under a fluorescent microscope (Zeiss LSM510, USA). To confirm the haptotactic response of L-EPCs to OPN, serial concentrations of OPN (0, 0.1, and 1 µg/ml coating) were used and compared to FN as a positive control. Data from three independent experiments were averaged and significance was determined by *t*-Test for haptotaxis versus chemotaxis. Slopes were determined for the haptotaxis effects of

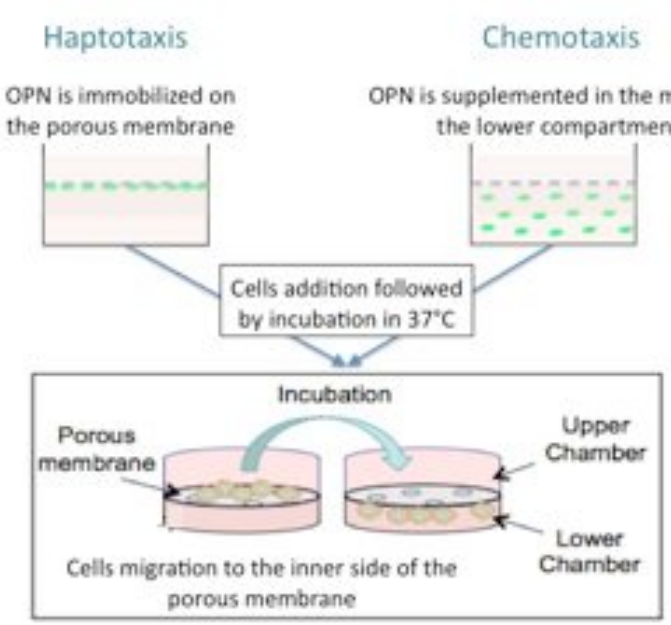

FIGURE 3: Haptotaxis and chemotaxis migration in Boyden chamber inserts.

OPN and FN concentrations.

2.5. Barrier Migration Assay:

This was performed according to Kroening and Goppelt-Struebe (2010) with slight changes. After coating 24 well plates as previously indicated in Section 2.2 with 0, 1, 10, 100 µM of OPN or FN in PBS overnight, migration inserts (CytoSelect,

cellbiolabs, USA) were applied gently and were kept stationary to prevent scratching, see (***Figure 4)***. Confluent layers of L-EPC were incubated in 2% serum media one day before the assay. Next day, L-EPCs were detached using TrypLE™. After 10 min, TrypLE™ was neutralized with 20% serum complete media and cell suspensions were centrifuged at 220×g for 5 min. Then, supernatant was removed and cells re-suspended in 5 ml of PBS and re-centrifuged at 220 × g for 5 min. After that, 500 µl of 4×10^5 cells/ml in 2% serum media were added per well to allow spreading into a monolayer. Cells were then incubated for 4 h. After monitoring cell adhesion, inserts were removed gently and cells were washed with PBS then 2% serum media was added again and incubated for another 4 h. After the incubation, media was removed by inverting the plate onto an absorbent pad, and then cells were washed three times with PBS. For assessing cell migration, cells were fixed and stained with 0.5% Crystal Violet. Then, number of cell migrating in the area between the two leading edges of the wound was counted. Data were collected from two independent experiments.

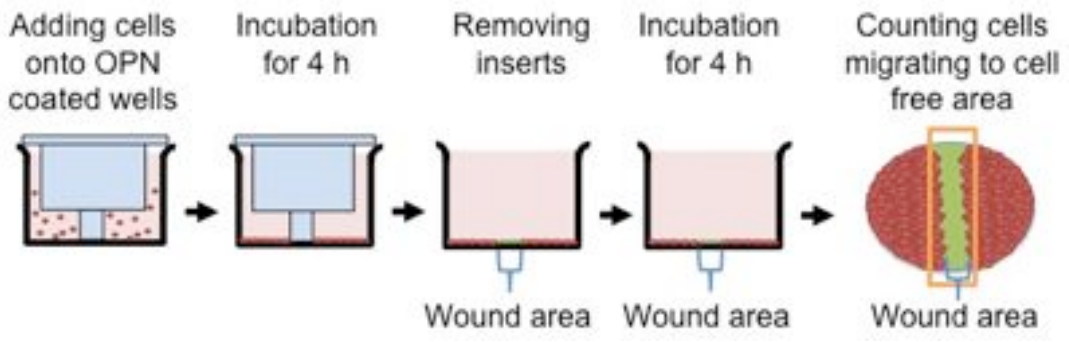

FIGURE 4: Barrier migration assay steps.

2.6. Shear Stress:

In vivo, EPCs are exposed to continuous flow created by blood circulation in the vasculature. An *in vitro* assay was applied to determine if OPN supports EPC adhesion and integrity under flow conditions. For this purpose, an special attachment to the ECIS instrument (Applied Biophysics, USA) was used. As described above, this instrument electrically monitors tissue culture by measuring the impedance of cells cultured on small gold film electrodes (8F1E, Applied Biophysics, USA). The readings were collected in real time, every 2 min. An assay similar to that developed by DePaola, Phelps et al. (2001) was employed . Wells were either coated with 10μM of OPN, or kept uncoated in 0.1M NaCl overnight as indicated in Section 2.2. Next day, the assay was started by seeding 100 μl of 1×10^7 cells/ml into the ECIS wells. Cells were allowed to adhere for 4 h. After that, OPN/flow or uncoated/flow chambers were inserted into the monitoring station and connected to the flow circuit. The machine was run for 15 min with flow *off* to ensure stability; readings were calibrated to 50 nanofarads capacitance. Then, flow was initiated by applying a flow rate 8ml/min producing a calculated 10 dynes shear stress. For OPN/static condition, chambers were inserted into the monitoring station without connection to the flow circuit for the whole experimental period. Measurements were obtained using a frequency of 4000 HZ, which is a moderate frequency that can measure both the fraction of surface covered by cells as well as cell-cell contact. Laminar flow was applied for 12 h. Data from four, two, and three independent experiments for OPN/flow, uncoated/flow, and OPN static conditions respectively, were averaged and normalized per each condition.

2.7. Receptor Blocking:

OPN binds to CD44 and many β1 integrins that mediate cell adhesion to the RGD motif. In addition results of an RNA micro assay (Appendix) showed that L-EPCs express CD44 at high level; and that β1 integrin binding protein mRNA was increased when cells were seeded on OPN compared to an uncoated substrate. Thus, this assay was applied to determine if OPN binds through these two receptors to L-EPCs. The experiment started by coating 24 well plates with 10 μM OPN in PBS as indicated in Section 2.2. A confluent layer of L-EPCs was incubated in 2% serum media one day before the assay. Next day, L-EPCs were detached using TrypLE™. After 10 min, TrypLE™ was neutralized with 20% serum complete media and cell suspensions were centrifuged at 220×g for 5 min. The supernatant was then removed and cells were re-suspended in 5 ml of PBS and re-centrifuged at 220×g for 5 min. After that, 100 μl of 5×10^4 cells/ml in 2% serum media were incubated for 30 min at room temperature with 5 μl of either a CD44 blocking antibody (R&D, USA), or β1 integrin blocking antibody (Santa Cruz, USA), or IgG isotype (Cell Signaling, USA). At the end of the antibody incubation, cells were re-suspended with 400 μl of 2% media and added into the coated wells then incubated at 37°C for 4 hours. Media was then removed by inverting the plate onto an absorbent pad, and the cells were washed three times with PBS, and then fixed with 4% paraformaldehyde for 10 min at room temperature. The fixative solution was removed and wells were washed three times with cold PBS. Cells were stained with 0.5% Crystal Violet for 30 min at room temperature. The wells were then washed three times with ddH2O and allowed to dry overnight. Adherent cells were counted using phase contrast microscopy at 20X in 4 fields and percentage of adherent cells was calculated versus unblocked receptors condition, and averaged per each well. Data from 3 independent experiments were

averaged and then data significance was determined with Dunnet's test.

2.8. Western Blot:

The Rho GTPase family was shown to play a role in maintaining cell integrity (Beckers, van Hinsbergh et al. 2010). In addition, data from RNA micro array showed up-regulation of mRNA expression of GTPase (Appendix). Here, we focused on Cdc42/Rac/RhoA protein expression in L-EPCs seeded on OPN, with or without CD44, and β1 integrin blocking. L-EPCs seeded on uncoated surfaces served as controls. Coatings were prepared as indicated in section 2.2. The experiment started by reducing the serum in EBM-2 to 2% serum media in a confluent layer of L-EPCs one day before the assay. Next day, L-EPCs were detached using TrypLE™. After 10 min, TrypLE™ was neutralized with 20% serum complete media and cell suspensions were centrifuged at 220×g for 5 min. Then, supernatant was removed and cells were re-suspended in 5 ml of PBS and re-centrifuged at 220×g for 5 min. After that, 500µl of 5×10^5 cells/ ml in 2% serum media were added into 10µM OPN coated or non-coated plates and incubated at 37°C for 4 hours. At the end of the incubation, media was removed and wells were washed three times with cold PBS to remove residual proteins from media. Total cells proteins were extracted using 50µl of cold RIPA buffer on ice. Cell extracts were transferred to an Eppendorf tube for each condition, and centrifuged at 220×g for 20 min at 4ºC. Supernatant was collected and protein concentrations were determined directly with BSA method at 560 nm, or stored at -20 until use. For electophoresis, 30µg of total proteins were loaded into each well of a 10% SDS PAGE gel at 85 volt for 105 min in a mini gel electrophoresis apparatus (Biorad, USA). Then, proteins were transferred to PVDF (Millipore, USA)

membrane, after activation with methanol, using a semi-dry transfer apparatus (fisher, USA) at 2mAmp/ cm^2 of the membrane for 45 min. After that, membranes were stained with ponceau-s-red stain to ensure protein transfer success. Then, membranes were blotted with an antibody specific for active GTPase (Cdc42/ Rac/ RhoA) at a concentration of 1:500 in 5% BSA Tris buffer (Cell Signaling, USA) overnight at 4ºC, or an antibody for total Cdc42/ Rac or Rho A (Cell Signaling, USA) at a concentration of 1:1000 in 5% BSA Tris buffer at room temperature for 1 hour. Proteins were detected by incubating membranes after each 1ºantibody with horseradish peroxidase HRP secondary antibody (Cell Signaling, USA) for 30 min. Bands were detected with ECL solution (Healthcare, USA). Average change in Cdc42/ Rac or RhoA activation was calculated by measuring western blot band intensity from three independent experiments (using ImageJ software, USA), and calculating the ratio versus total protein band intensities. Data were averaged and data significance was determined with Dunnet's test.

3. Results

3.1. Adhesion of L-EPCs to OPN substrates

EPCs have previously been shown to mobilize from the bone marrow into the blood stream, but failed to adhere to site of injury in OPN null mice (Leen, Filipe et al. 2008). We therefore determined whether OPN is an adhesive substrate for L-EPCs, and if so, whether the effect was dose-dependent. Here, L-EPCs were seeded on serial concentrations of OPN coatings for 4 h. Then, wells were washed and attached cells were stained with Crystal violet and counted under a 20X objective. Log scale results shown in ***Figure 5: A*** shows a dose-dependent increase of L-EPC adhesion to OPN (39.5±3.6, 73.6±1.7, 88.4±1.7, and 111.9±6 cells/field for 0, 1, 10, and 100 μM OPN coating concentrations, respectively). Statistically significant dose dependence was determined by one way ANOVA ***p< 0.0001. Also, the correlative relationship between data means and OPN concentrations was determined by regression analysis, R^2 value of 0.9.

A similar proportional effect of OPN concentrations was also observed on the percentage of L-EPC spreading (***Figure 5: B)***. L-EPC spreading was determined by calculating the area of adhering cells, ***Figure 5: A*** with image analysis software (Digital sight DS-L2 control unite); cells with an area of more than 1500 μm^2 (spread cells) were counted in 4 fields per well under a 40X objective. The percentage of, spread cells was calculated and averaged per each well. L-EPC spreading percentages compared to the total number of cells are 38.1±4.5, 58.7±0.9, 66.1±2.5, and 80.2±3.6% for 0 μM, 1 μM, 10 μM, and 100 μM OPN coatings, respectively. Dose dependence was determined by calculating the correlation of OPN concentrations to percentage spreading, R^2=0.9

L-EPC adhesion to 10 μM OPN was also compared to 10 μM FN ***(Figure 6)***. The measurements were taken using ECIS, where cell adhesion increases resistance to the flow of electrical current (described in more detail in Section 2.6). Readings of resistance were taken at 0, 5, 10, 15, and 20 h, respectively are 244.3±8.7, 649.3±30.0, 1011.5±159.1, 1166.6±196 and 1265.3±192.4 for cells adhering to OPN; and, 259.0, 966.0, 1192.0, 1455 and 1507.0, for cells adhering to FN. The results were also compared to L-EPC adhesion to uncoated plates (231.5, 392.0, 476.0, 460.5 and 469.5). Data were obtained from 6, 2, and 2 independent experiments for OPN coated, FN coated, and uncoated surfaces, respectively. Significance correlation between time and resistance readings was determined in OPN treated conditions, and shows R^2 of 0.93. Briefly, immobilized OPN induced L-EPC adhesion in a time-dependent manner.

3.2. OPN induced haptotactic migration of L-EPC:

Both immobilized and soluble OPN were shown to induce cell migration previously in cell types other than L-EPCs (Liaw, Almeida et al. 1994; Duvall, Weiss et al. 2008; Buback, Renkl et al. 2009). In order to assess if OPN induces L-EPC migration, immobilized and soluble forms of OPN were used to examine L-EPC directional migration by haptotaxis, and chemotaxis, respectively ***(Fgure 7: A)***. The data were collected by counting total number of cells that had migrated to the inner side of the Boyden chamber membrane. Results show that the number of haptotaxis-migrated L-EPCs are significantly higher $^{**}p \leq 0.01$ than that produced by the chemotactic stimuli, where the number of migrated cells was 154±12.3 compared to 49±1.7 cells/ area, for haptotaxis and chemotaxis migration, respectively. To confirm the haptotactic response of L-EPCs to OPN, serial concentrations of OPN coating

were used and compared to FN as a positive control. The results in ***Fgure 7: B*** show a proportional relationship between OPN concentration and cell migration, as indicated by the data: 162±31, 46.5±4.5, and 40±10 cells/area, r= 0.9 for 1, 0.1, and 0 µl/ml, respectively. The data also show that the number of migrated L-EPCs was 162, 85, and 40±10 cells / area toward 1, 0.1, and 0 µl /ml FN respectively, r = 0.9. Micromotion tests shown in ***Figure 7: C*** were applied to identify if OPN induces directional migration only, or also stimulates cell migration toward cell-free areas. Even though the results were insignificant for L-EPCs seeded on OPN, the results showed a protein concentration-dependent migration of 70±2.8, 50±1.2, 37±1.5, and 29.25±1.5 cells/area. R^2 = 0.4 for 100, 10, 1, and 0 µM OPN, versus 153±9.4, 108 ±2.27, 95.25± 3.3, and 29.25±1.5, R^2 = 0.8 for 100, 10, 1, and 0 µM FN, respectively.

3.3. OPN promoted cell integrity and resistance to shear stress induced by laminar flow:

Because EPCs are exposed to flow created by blood flow *in vivo* (Hur, Yoon et al. 2004; Ingram, Mead et al. 2005), it was crucial to test if L-EPC adhesion to OPN could increase endothelium layer integrity under flow conditions. Three conditions were tested in this experiment: L-EPCs seeded on OPN and exposed to flow, L-EPCs seeded on uncoated surface and exposed to flow, and L-EPCs seeded on OPN in static conditions. In the ECIS laminar flow chambers, resistance readings represent the flow of electrical current between the ventral surface of the cells and substratum, as well as intercellular gaps of the monolayer. In other words, the closer the contact of cell-cell or cell-substratum, the more resistance will be encountered in the electrical flow between the electrode and media, which is used as an electrolyte. The results ***(Figure 8)*** show that upon start of the flow, which produces a laminar shear stress of approximately 10 dynes/cm^2, the resistance readings of L-EPCs seeded

on OPN increased dramatically up to 2.5 h, then persisted at high readings for 12 h. This reading was significantly higher than that observed for cells seeded on an uncoated surface exposed to the same shear stress for 12 h. Both flow conditions showed an increasing trend of resistance compared to cells seeded on OPN in static conditions, which showed a slight increase up to 5 h, where it formed a plateau followed by a decrease starting at 7.5 h. Statistical significance was determined by calculating the slopes for the 245 readings in the three conditions as 642.8±16.53, 290±2.88, and 62.84±8.83, for OPN/flow, uncoated/flow, and OPN coated/static, respectively. The elevation of resistance in the condition OPN/flow could be a result of the increased adhesion of L-EPCs compared to the uncoated surface, which can produce more integrity of the L-EPCs layer and thereby more resistance to detachment by flow shear force. In conclusion, OPN induces cell adhesion, most likely by allowing cells to integrate and resist detachments when exposed to shear force. This supports the essential function of OPN as an adhesive protein for EPCs *in vivo*.

3.4. CD44 and β-1 integrin are involved in L-EPC adhesion to OPN:

RNA microarray analysis (Appendix) revealed that EPCs highly express CD44, and that stimulation by OPN enhances RNA expression of β1 integrin binding protein. Accordingly, CD44 as well as β-1 integrin involvement was examined ***(Figure 9)***. Adhesion of L-EPCs to 10 μM OPN after individual blocking of CD44, or β1 integrin, or both with blocking antibodies were compared with L-EPCs blocked with IgG isotype as a negative control. The results showed that by comparing the percentage of cells adhering to OPN, individual blocking of CD44 or β1 integrin had significantly reduced L-EPCs adhesion to OPN indicated by 48.4±11.4%, and 45.08±10.5%

respectively, **p≤ 0.01. Even more significant reduction was observed by dual blocking of both receptors compared to the IgG isotype control (33.71±8.4% *** p≤ 0.001). However, the CD44 and β1 integrin blocking was not able to completely abolish the adhesion of L-EPCs to the OPN-coated surface. This might be an indicator that L-EPCs adhere also through other fundamental receptors. In conclusion, the results showed that both receptors CD44 and β-1 integrin are involved in mediating L-EPC adhesion to OPN.

3.5. Rho family GTPases are activated by OPN through CD44 and β-1 integrin:

Rho family GTPases are involved in maintaining cell integrity (Price, Leng et al. 1998; Filipenko, Attwell et al. 2005; Beckers, van Hinsbergh et al. 2010). The RNA microarray data obtained showed that the RNA of Rho family GTPases was up-regulated under OPN treatment. Thus, the activation of Rho family GTPases is crucial to characterize the adhesive function of OPN, and its role in L-EPC integrity. Western blots of proteins isolated from cells seeded on OPN-coated surfaces were obtained for CD44- and β1 integrin-blocked and unblocked cells ***(Figure 10: B)***. Protein intensities of phosphorylated proteins versus total proteins, showed that L-EPCs seeded on OPN showed a 3-fold increase in Cdc42/Rac/RhoA activation ($p < 0.05$), over L-EPCs plated on uncoated plastic ***(Figure 10: A)***. In addition, this activation of Cdc42/Rac/RhoA was also dependent on the interaction between CD44 and β1 integrin with OPN, as the activation of Cdc42/Rac/RhoA in both CD44- and β1 integrin-blocked cells was decreased compared to unblocked receptor cells, with intensity measurements at 2.17±0.6, and 2.06±0.4 for both CD44 and β1 integrin, respectively. However, blocking of CD44 and β1 integrin did not show any statistically significant difference compared to unblocked L-EPC, suggesting that the

activation of Cdc42/Rac/RhoA may be conducted through both CD44 or β1 integrin adhesion or by an as yet unknown adhesion pathway. This identifies a limitation of this assay, where we only looked at CD44 and β1 integrin, and that there might be other important receptors involved in this process.

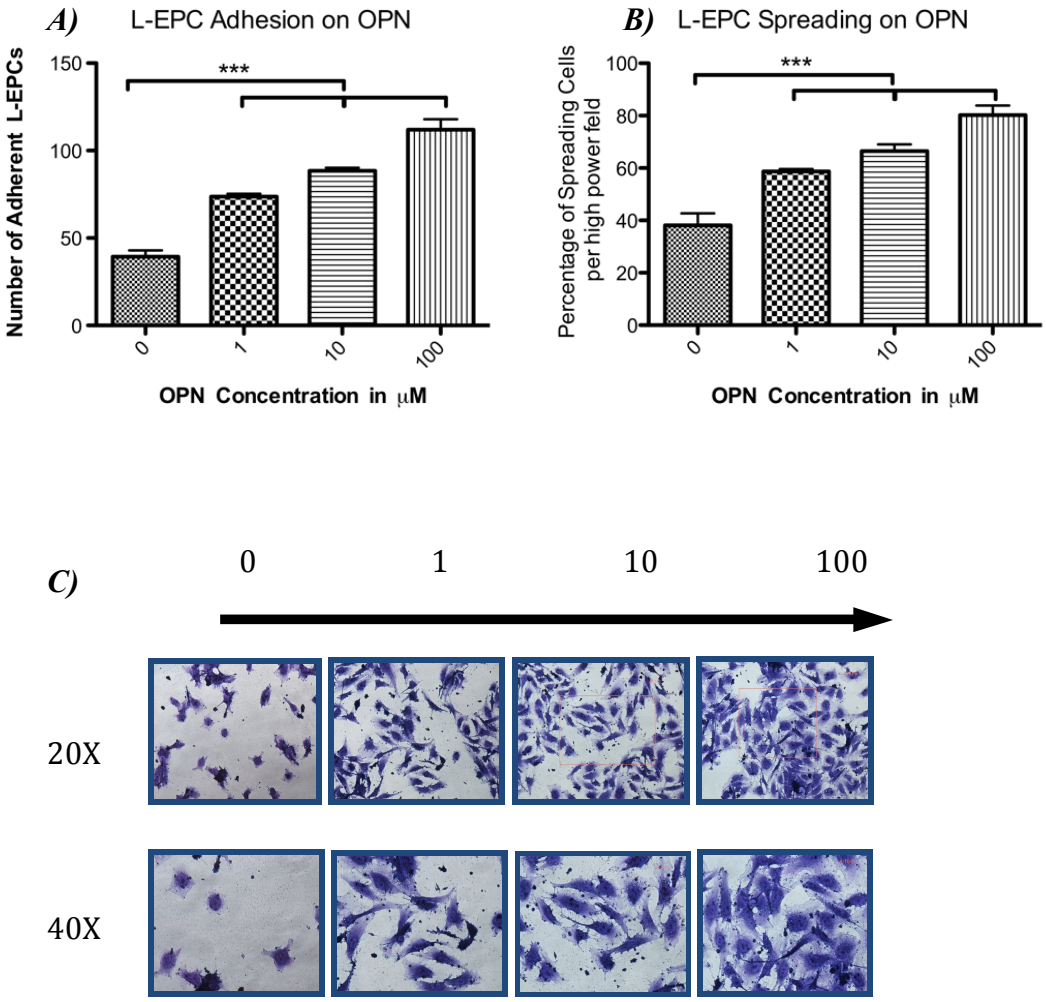

FIGURE 5: Adhesion and spreading of human L-EPCs on osteopontin adsorbed onto polystyrene. 500 µl of 5× 10^3 cells/ ml of serum free media were plated onto wells coated with 100, 10, 1, or 0 µM of OPN. *(A)* Number of adherent L-EPCs on different concentrations of OPN. Each bar represents the counting of adherent cells in four fields per well. One way ANOVA analysis shows ***p< 0.0001, and R^2= 0.9 *(B)* Percentage of spreading L-EPCs after incubation for four hours on different concentrations of OPN at 37°C. Each bar represents the percentage of spreading cells from the total number of adherent cells in four fields per well. The result represents the mean ± SEM from one experiment. Statistical significance of differences amongst groups was determined by one way ANOVA ***p< 0.0001, and R^2= 0.9 *(C)* Images of the crystal violet stained adherent cells under 20X and 40X magnification power.

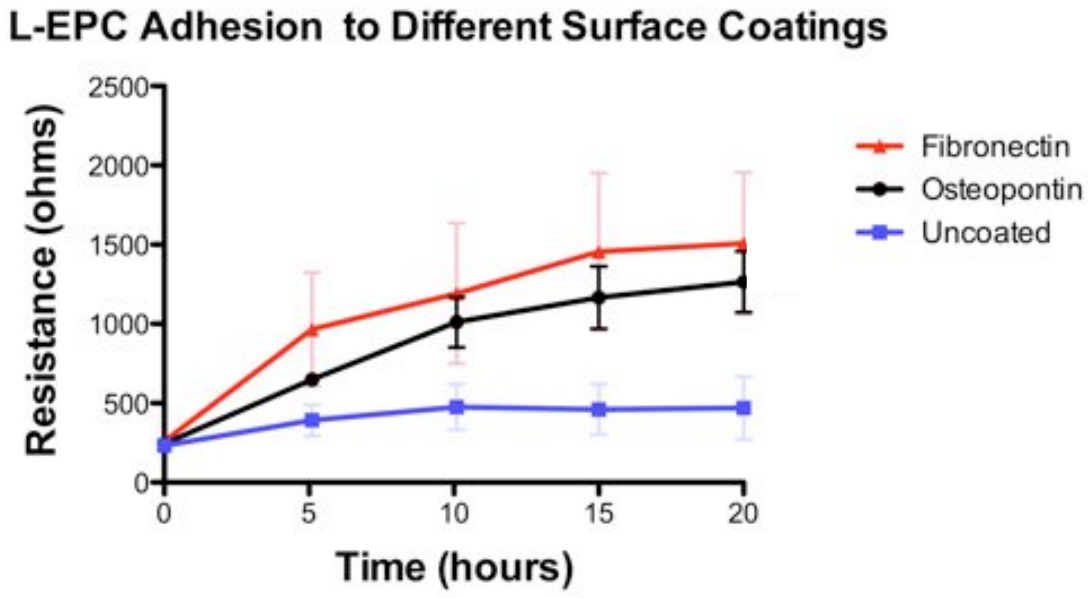

FIGURE 6: L-EPC adhesion to different surface coatings. Gold electrodes were either coated with 10 µM of OPNor FN, or left uncoated. After calibration with cell-free media, 400 µl of 5×10^3 cells/ml were added. The graph shows comparison of cell resistance versus time in hours, when seeded on OPN, and compared with FN and uncoated gold electrodes. The measurements of resistance were collected at a frequency of 4000 Hz in ohms for 20 hours. Data reported were taken from 6, 2, and 2 independent experiments, and significance correlation between time and resistance reading was determined in OPN and shows R^2 of 0.93.

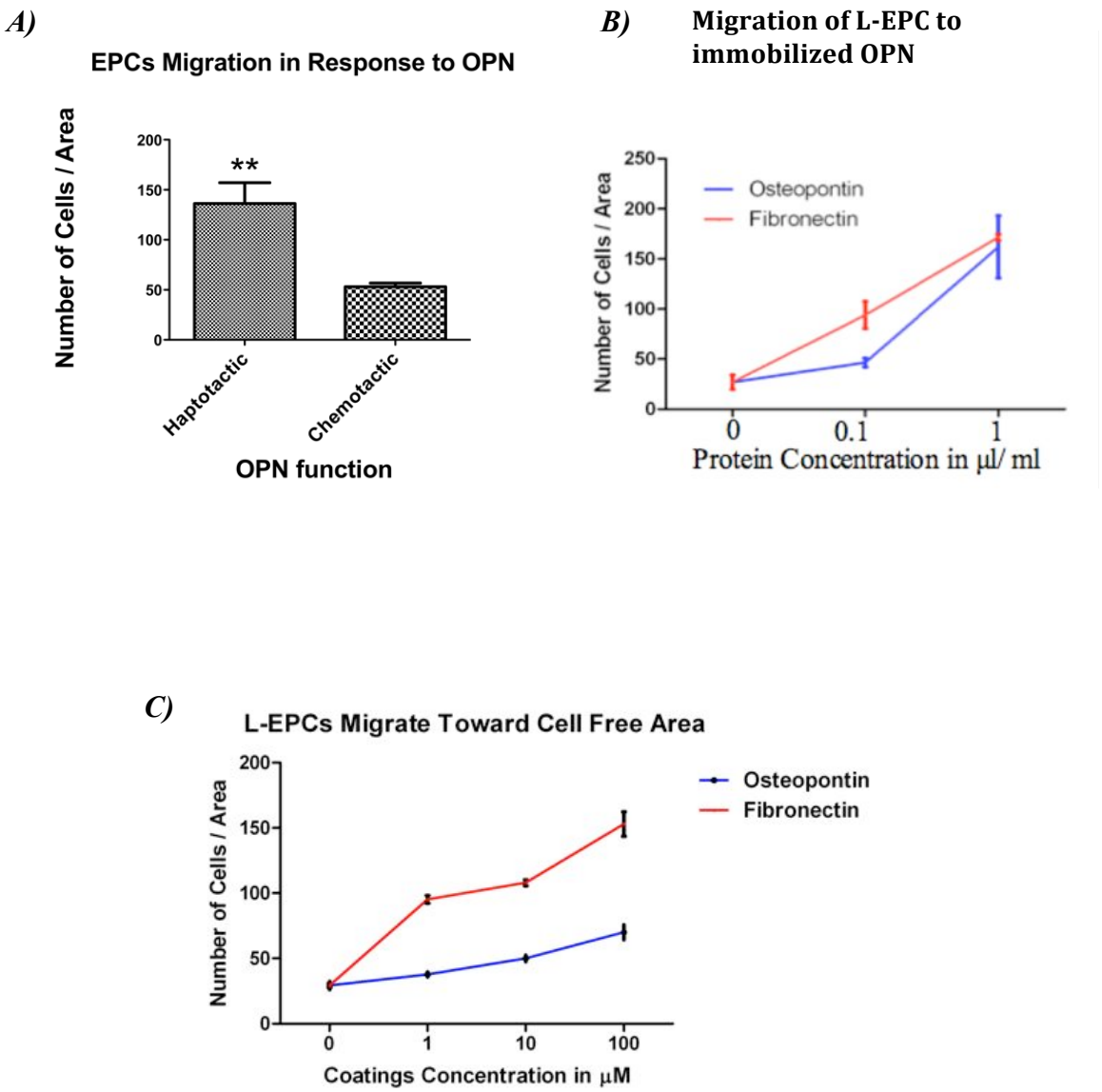

FIGURE 7: OPN induces haptotactic migration in L-EPCs. *(A)* The number of migrated L- EPCs per area; Boyden chamber membranes were either coated (Haptotactic) or uncoated (chemotactic) with 1µl/ml OPN, **p≤ 0.01 by student *t* test. *(B)* The number of migrated L-EPCs per area; Boyden chamber membranes were coated with either OPN or FN at 0, 0.1, and 1 µl/ml. *(C)* shows the number of L-EPCs migrated between the two leading edges of wound made by inserts; surfaces were coated with either OPN or FN at 0, 1, 10, and 100 µM. the correlation between cell number and protein coating concentration shows R^2 = 0.4 for OPN treated cells and R^2 = 0.8 for FN treated cells. Data points represent mean± SEM.

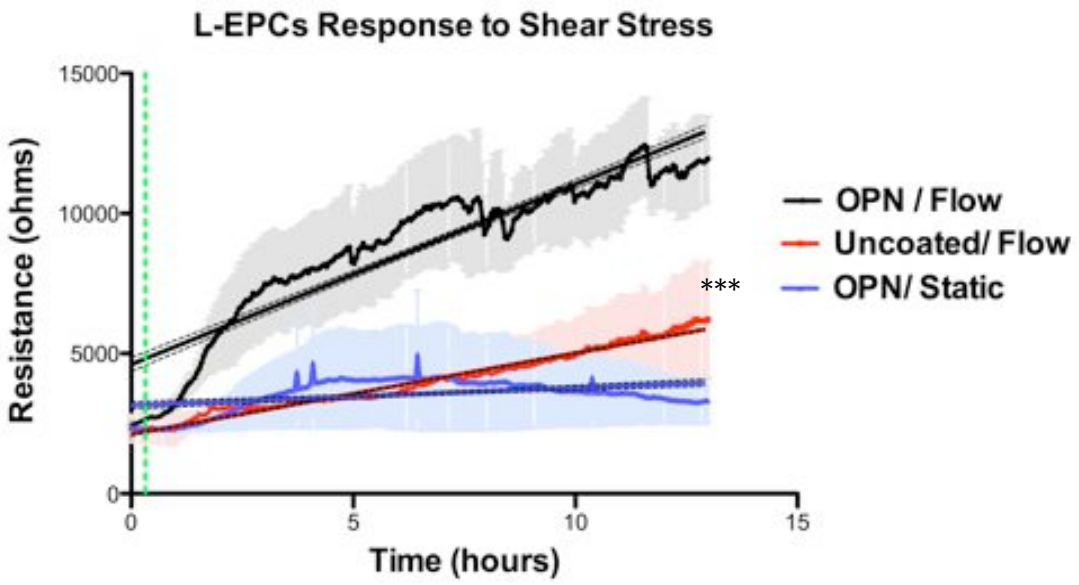

FIGURE 8: OPN induces L-EPC integrity and resistance to shear stress force. Comparison of L-EPC resistance in the following conditions: under flow (10 dynes shear stress) when seeded on OPN or uncoated surface or on OPN when exposed to flow or static conditions. 100 µl of 10^7 of L-EPCs in serum reduced (2% in EBM) media, were inoculated in ECIS specialized flow chamber slides, and allowed to adhere for four hours. Measurements started with no flow for 15 min and were taken under a frequency of 4000Hz until 12 hours. The result shows significant correlation of resistance readings to the time as slopes were (642.8±16.53, 290±2.88, and 62.84±8.83; statistical significance was seen between OPN/ flow and other two conditions ***$p \leq 0.001$).

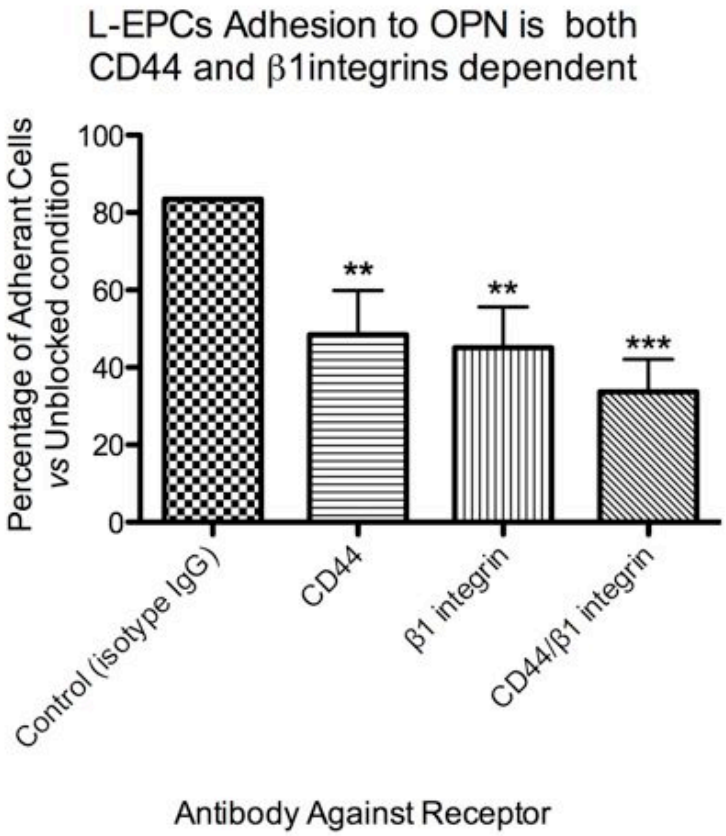

FIGURE 9: OPN binds to L-EPC through but not limited to CD44/ β-1 integrin. Adhesion of L-EPCs to osteopontin adsorbed onto polystyrene. 500 µl of 3×10^3 cells/ ml of 2% serum media were plated onto wells coated with 10 µM of OPN. Cells were plated either after blocking CD44 or β-1 integrin and IgG isotype for 30 minutes. The results were 48.4±11.4%, 45.08±10.5%, and 33.71±8.4%; **p≤ 0.01, *** p≤ 0.001 for CD44, β-1 integrin, and CD44/ β-1 integrin respectively. Each bar represents mean ± SEM of the percentage of adherent cells *versus* the unblocked condition in four fields per well at 20X and significance was determined by the Dunnett's test.

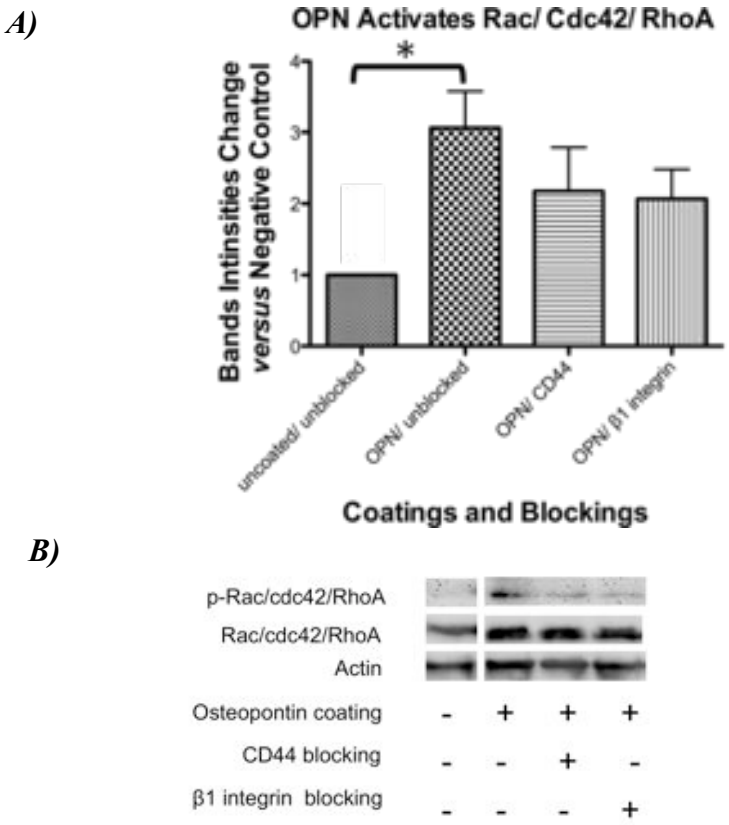

FIGURE 10: OPN activates GTPases: Cdc42, Rac, and RhoA in L-EPCs through CD44, and β1 integrin. 5 ml in 5×10^4 cells/ ml of 2% serum media were plated onto wells coated with 0, or 10 μM of OPN. Cells were plated either after blocking CD44 or β1 integrin or left unblocked before seeding. After seeding, cells were incubated up to four hours, and then lysed with RIPA buffer. Proteins were separated on 10% SDS PAGE gels. (A) relative intensity of protein bands on western blot in the different conditions versus the unblocked condition was determined using ImageJ software. Data were significant between OPN and uncoated surface conditions as (3.06±0.5, and 1.00±0.0 respectively, *$p \leq 0.05$ by Dunnet's test). However, blocking of CD44 and β1 integrin did not show any significance to OPN/ unblocked condition (2.17±0.6, and 2.06±0.4) for both CD44 and β1 integrin respectively. Significance was determined by Dunnet's test. (B) Western blot of proteins from cells seeded on OPN with or without pretreatment with CD44 or β1 integrin.

4. Discussion

Endothelial integrity is crucial for preservation of normal function of the cardiovascular system (Sumpio, Riley et al. 2002; Infanger, Shakibaei et al. 2005; Huang, Hou et al. 2007; Xu 2007). EPCs play a crucial role in vascular regeneration and re-endothelialization. These cells are mobilized from bone marrow, moving into the peripheral blood circulation to the site of injury, where they differentiate into a mature endothelium lineage (Xu 2007; Wang, Lin et al. 2009; Yin, Zhao et al. 2010; Liu, Li et al. 2011). This process involves the collaboration of a number of variables, including response to growth factors and cytokines secreted at the site of injury. Leen et al. (2008) demonstrated that OPN was involved in this process. Even though the specific role of OPN was not defined, they showed the importance of OPN in estrogen (E2)-enhanced endothelial repair. This study indicated that the number of bone marrow-derived cells mobilized into the blood stream did not differ between wild-type mice (OPN+/+) or OPN-deficient mice (OPN-/-). However, endothelial repair was lost in OPN-/- mice. Leen and his colleagues also reported OPN was expressed more highly in the wound periphery of an injured artery in wild-type mice compared to uninjured vessels. OPN overexpression was also correlated with increased endothelial repair and MNC incorporation into the wounded area (Leen, Filipe et al. 2008; Molin, van den Akker et al. 2008). Thus, we can infer that OPN works by mediating cell adhesion to wound areas. Our study had aimed to determine the in vitro effects of OPN on EPCs, focusing on the adhesive effect of OPN on L-EPCs. We demonstrated that OPN induces adhesion and spreading of L-EPCs in a dose dependent manner. Furthermore, we showed that OPN induced haptotactic rather than chemotactic migration, and that the haptotaxis of L-EPCs was OPN concentration dependent. In addition, the adhesion induced by OPN also promoted L-

EPC integrity and resistance to detachment by flow shear force. Finally, adhesion to OPN induced GTPase activation. The adhesion was shown to occur in part through binding of OPN to CD44 and β1 integrin, but was not dependent on these two receptors.

Although the exact functions of EPCs subtypes are not fully defined, we used L-EPCs in this project. These cells were so named because of their late-emergence from the MNCs culture (after 2 to 3 weeks) in vitro as proliferative adherent cells with cobblestone appearance (Ingram, Mead et al. 2004). The reason for choosing L-EPCs in this project is not only because of their ability to form a netlike structure *in vitro* but because their morphology, markers, functional protein expression and growth characteristics better resemble those of ECs than early-EPCs. L-EPCs can form blood vessels when implanted in matrix scaffolds in animal models and become a part of the systemic circulation of the host (Melero-Martin, Khan et al. 2007; Yoder, Mead et al. 2007; Au, Daheron et al. 2008). In addition, two recent studies reported the ability of L-EPCs to incorporate into vasculature and restore blood flow into avascularized areas. Dubois et al. (2010) reported that transplantation of L-EPCs into pig models after acute myocardial infarction resulted in substantial improvement in myocardial infarct remodeling and heart function through direct incorporation of these cells into the endothelium (Dubois, Liu et al. 2010). In the study by Medina and coworkers (2010), they reported that human L-EPCs directly incorporated into vasculature after induction of retinal ischaemia in murine models, significantly enhancing normovascular areas (Medina, O'Neill et al. 2010). Thus, by the characteristics and functional capacity of L-EPCs we can conclude that these cells are capable of filling gaps of endothelial wound areas after injury.

BIOLOGICAL EFFECTS OF OPN ON EPCs

Leen and his colleagues (2008) were the first group to illustrate the fundamental role of OPN in endothelium repair and MNC incorporation into the wounded area (Leen, Filipe et al. 2008; Molin, van den Akker et al. 2008). The subsequent study by O'Brien and coworkers (2009) evaluated the role of OPN in inducing the angiogenic function of EPCs from OPN knockout mice. They reported that EPCs from OPN knockout mice showed a significantly lower number of tubules compared to wild-type mice; this reduction was recovered when the cells were pre-incubated with recombinant OPN. Interestingly, they also found that conditioned media from wild-type cells and recombinant OPN pre-incubated knockout EPCs could induce EPC tubule formation. Both cellular conditions expressed interleukin-6 (IL-6) and fibroblast growth factor (FGF) at a higher level than did OPN knockout EPCs. (Vaughan, Duffy et al. 2009). More recently a study by Yu *et al*. (2011) focused on the functional activity of OPN on L-EPCs isolated from umbilical cord MNCs. They reported that exposure to OPN inhibits L-EPC proliferation, adhesion to FN as well as their *in vitro* vasculogenesis capacity in a dose dependent manner. However, OPN increases migratory activity of late EPCs toward VEGF (Yu, Liu et al. 2011). However, none of these studies showed the role of OPN in the EPCs adhesion and the integrity of EPCs layer.

Homing of cells is mediated through both recruitment and adhesion of cells to the site of injury. OPN was reported as a matricellular protein secreted by ECs and SMCs after injury. OPN was determined to have a vital role in MNCs, which include EPCs, in adhesion and healing of vascular injury. However, the mechanism by which OPN is involved in EPC-enhanced re-endothelialization has yet to be determined. Here, we determined the adhesion effect of OPN by its ability to mediate L-EPC adhesion and spreading and that these two processes were dose dependent. OPN also played a role

in mediating cellular haptotactic migration in a dose dependent manner. In line with our results, Leali and colleagues (2007) reported that in murine aortic endothelial cells OPN was essential for vascular endothelial cell adhesion. When transfected with OPN cDNA, these cells had both strong adhesion to and spreading on immobilized OPN. In addition, OPN reduced endothelial motility in the Boyden chamber assay, and reduced the ability of murine aortic endothelial cells to repair a wounded monolayer. Taken together, these data show that inhibition of cell motility by OPN is mediated through strong adhesion (Leali, Moroni et al. 2007). In addition, Nilsson and colleagues found that OPN is a key regulator for normal physiology of the HSC niche, which is also the precursor for endothelium tissue and its progenitors. OPN is responsible for keeping HSCs quiescent within endosteal bone surfaces, induction of primitive hematopoietic cell adhesion via β1 integrins, and suppression of primitive HPC proliferation *in vitro* (Nilsson, Johnston et al. 2005).

L-EPCs were also shown to migrate toward OPN but motility on OPN coatings has not been previously demonstrated. Fom the Boyden chamber assay, we found that the migration represented haptotaxis rather than chemotaxis. Two explanations exist for this phenomenon. First, it might be due to the retention of OPN on the coatings, in which retained OPN is then available to bind to OPN receptors on the surface of L-EPCs, initiating their movement toward the OPN coated area. Second, it might be that soluble OPN induces cell survival and independence of adhesion. In other studies, OPN acted as a recruitment protein to bring hematopoietic cells to the site of inflammation (Scatena, Liaw et al. 2007; Buback, Renkl et al. 2009). A recent study showed that stimulation of L-EPCs by OPN increases migration toward VEGF through up-regulating VEGF Receptor II (KDR) (Yu, Liu et al. 2011). Interestingly, both VEGF and OPN were found at wound edges of regenerating

endothelium (Senger, Ledbetter et al. 1996; Infanger, Shakibaei et al. 2005), indicating that their attraction of L-EPCs could play a role in wound healing and OPN had no role in mediating cell chemotaxis (Leen, Filipe et al. 2008). In addition, a recent report showed that *in vitro*, OPN mediates acceleration of re-endothelialization and endothelial repair (Liaw, Lindner et al. 1995). However, this acceleration only occurred at low concentrations, while overexpression dramatically impairs re-endothelialization by inhibiting EC motility and promoting strong adhesions (Leali, Moroni et al. 2007). Taken together, the data suggest that OPN mediated the haptotaxis of L-EPCs through its adhesive function, while chemotactic recruitment is mediated through increasing KDR expression for VEGF.

EPCs and endothelial cells in the vascular wall are subjected to continuous shear forces created by the flow of blood through the vessels. One goal of this study was to determine if OPN could support cell integrity and resist detachment under flow conditions. Our results showed that cells seeded on OPN and exposed to shear stress forces were highly resistant to detachment (***Figure 8***), indicating increased cell-cell and cell-matrix adhesion. We inferred that the resistance to detachment was due to the ability of OPN to rapidly induce firm EPC adhesion at the cell-substrate interface (***Figure 6).*** The strong focal adhesion was most likely due to the activation of Rho GTPases (***Figure 10)***. This process generates a confluent layer that could withstand shear stress. On the other hand, shear stress can induce mechanotransduction and the expression of potent biological mediators one of which is eNOS, which expression may induce enhanced cell survival (Kolluru, Sinha et al. 2010). This might be the reason why even the uncoated / flow condition promoted more cell survival than the OPN / static condition.

BIOLOGICAL EFFECTS OF OPN ON EPCs

The use of OPN as a coating for vascular biomaterial implants could have a number of advantages in particular it may promote regenerative cell recruitment, survival, and rapid endothleliazation of the flow surface. Several coatings have been used so far in the field of biomaterial coatings; these include specific antibodies such as anti-CD34 or anti-KDR, RGD peptides, polymers, or proteins (Dennis Bruemmer, Alan R. Collins et al. 2003). However, what makes OPN even more appropriate for coatings is because of its wound specific expression, by which OPN will not only mediate strong adhesion (Malmstrom, Christensen et al. 2010), but may also mediate neovascularization and the formation of vascular networks in tissue implants (Asou, Rittling et al. 2001; Liu, Chen et al. 2008). OPN may be more biologically relevant in wound healing processes than the use of antibodies as OPN has multiple binding sites, and can promote cell signaling CD44 (Liaw, Lindner et al. 1995; Barry, Ludbrook et al. 2000). In addition, OPN cleavage by proteases (such as thrombin) released at the wound site can produce a more active form of OPN with additional epitopes for cell interaction. On the other hand, OPN is not a selective protein, i.e. it can affect several types of cells including monocytes, mesenchymal stem cells MSCs (Hakimzadeh, Stewart et al. 2010), endothelial cells, and SMCs (Liaw, Almeida et al. 1994). OPN has been demonstrated to be involved in disease progression in atherosclerotic animal models, yet these effects appear limited to monocyte specific expression of OPN (Dennis Bruemmer, Alan R. Collins et al. 2003). Thus as with many matricllular proteins it is the limited spatial localization of OPN that may prove beneficial and any potential therapy needs to strike an appropriate balance in the site specific delivery and immobilization of this matricellular protein.

Full-length OPN activates a wide variety of receptors including CD44 variants and integrins (Denhardt, Giachelli et al. 2001; Scatena, Liaw et al. 2007). We did not

evaluate the effect of cleaved forms of OPN, or the possibility that OPN may be cleaved by L-EPC secreted proteases such as MMP 2 and 9. Our data showed the ability of L-EPCs to respond to OPN was partially impaired when CD44 and β1 integrins were blocked. CD44 was highly expressed on cells used in this project, and is one of the main receptors of OPN. Upon binding to OPN, CD44 induces adhesion and migration of cells. Moreover, β1 integrin or fibronectin receptors induced cell adhesion to OPN through both RGD and SVVYGLR, as the number of adherent cells was reduced after pre-incubating L-EPCs with β1 integrin antibodies. However, blocking CD44 and β1 integrins did not inhibit activation of Rho GTPases, a group of proteins that control endothelium integrity (Beckers, van Hinsbergh et al. 2010). Western blot data showed that expression of RhoA GTPases (Rac, Cdc42, and RhoA) increased three times when EPCs were seeded on OPN-coated compared to uncoated surfaces, suggesting that OPN mediates adhesion and spreading of cells on protein coatings through the activation of these small GTPases. GTPases are responsible for the formation of stress fibers, lamellipodia and filopodia, and could induce formation of small substrate adhesions called focal complexes, which are involved in rearrangements of the actin cytoskeleton, and are partially responsible for the flattened morphology of the cells (Price, Leng et al. 1998; Filipenko, Attwell et al. 2005; Leali, Moroni et al. 2007). The incomplete inhibition of adhesion and Rho GTPase activation by blocking CD44, Beta-1 integrin, suggest that these data are limited since we only investigated CD44, Beta-1 integrin, Rac, Cdc42, RhoA activation.

Other receptors that can bind OPN and mediate adhesion of cells include αvβ1, α5β1, α4β1, α9β1, αvβ3, αvβ5, αvβ6, and α9β4 (Courter, Cao et al. ; Barry, Ludbrook et al. 2000; Barry, Ludbrook et al. 2000). If subjected to cleavage by cell

secreted proteases such as thrombin (Grassinger, Haylock et al. 2009), cathepsin D (Christensen, Schack et al. 2010), and MMP 3,5 and 12 (Gao, Agnihotri et al. 2004; Goncalves DaSilva, Liaw et al. 2010), cryptic sequences such as SVVYGLR will be exposed, displaying more functional capacities for OPN such as mediating cell migration, metastasis, and survival and inducing other signaling pathways including Akt, ERK1/2.

The data reported here were *in vitro* observations, limiting the ability to extrapolate the data to *in vivo* situations. Another dimension could have been reached by examining different forms of OPN, such as thrombin or MMP-cleaved, or transglutaminase-2 (TG2) polymerized OPN, as these forms were also shown to mediate more cell functions such as survival, adhesion, and migration. Nevertheless, the ability of OPN to mediate L-EPC adhesion, haptotactic migration and resistance to detachment under physiological flow shear force, suggests the feasibility of using OPN coatings to promote the re-endothelialization of biomaterial implants with L-EPCs.

5. References

Arroyo, A. G. and M. L. Iruela-Arispe (2010). "Extracellular matrix, inflammation, and the angiogenic response." Cardiovasc Res **86**(2): 226-235.

Asahara, T., H. Masuda, et al. (1999). "Bone marrow origin of endothelial progenitor cells responsible for postnatal vasculogenesis in physiological and pathological neovascularization." Circ Res **85**(3): 221-228.

Asahara, T., T. Takahashi, et al. (1999). "VEGF contributes to postnatal neovascularization by mobilizing bone marrow-derived endothelial progenitor cells." Embo J **18**(14): 3964-3972.

Asou, Y., S. R. Rittling, et al. (2001). "Osteopontin facilitates angiogenesis, accumulation of osteoclasts, and resorption in ectopic bone." Endocrinology **142**(3): 1325-1332.

Au, P., L. M. Daheron, et al. (2008). "Differential in vivo potential of endothelial progenitor cells from human umbilical cord blood and adult peripheral blood to form functional long-lasting vessels." Blood **111**(3): 1302-1305.

Barry, S. T., S. B. Ludbrook, et al. (2000). "Analysis of the alpha4beta1 integrin-osteopontin interaction." Exp Cell Res **258**(2): 342-351.

Barry, S. T., S. B. Ludbrook, et al. (2000). "A regulated interaction between alpha5beta1 integrin and osteopontin." Biochem Biophys Res Commun **267**(3): 764-769.

Beckers, C. M., V. W. van Hinsbergh, et al. (2010). "Driving Rho GTPase activity in endothelial cells regulates barrier integrity." Thromb Haemost **103**(1): 40-55.

Buback, F., A. C. Renkl, et al. (2009). "Osteopontin and the skin: multiple emerging roles in cutaneous biology and pathology." Exp Dermatol **18**(9): 750-759.

Calzi, S. L., M. B. Neu, et al. (2010). "Endothelial progenitor dysfunction in the pathogenesis of diabetic retinopathy: treatment concept to correct diabetes-associated deficits." Epma J **1**(1): 88-100.

Chavakis, E. and S. Dimmeler (2011). "Homing of Progenitor Cells to Ischemic Tissues." Antioxid Redox Signal.

Chavakis, E., C. Urbich, et al. (2008). "Homing and engraftment of progenitor cells: a prerequisite for cell therapy." J Mol Cell Cardiol **45**(4): 514-522.

Christensen, B., L. Schack, et al. (2010). "Osteopontin is cleaved at multiple sites close to its integrin-binding motifs in milk and is a novel substrate for plasmin and cathepsin D." J Biol Chem **285**(11): 7929-7937.

Courter, D., H. Cao, et al. (2010). "The RGD domain of human osteopontin promotes tumor growth and metastasis through activation of survival pathways." PLoS One **5**(3): e9633.

Dai, J., L. Peng, et al. (2009). "Osteopontin induces angiogenesis through activation of PI3K/AKT and ERK1/2 in endothelial cells." Oncogene **28**(38): 3412-3422.

Denhardt, D. T., C. M. Giachelli, et al. (2001). "Role of osteopontin in cellular signaling and toxicant injury." Annu Rev Pharmacol Toxicol **41**: 723-749.

DePaola, N., J. E. Phelps, et al. (2001). "Electrical impedance of cultured endothelium under fluid flow." Ann Biomed Eng **29**(8): 648-656.

Dhore, C. R., J. P. Cleutjens, et al. (2001). "Differential expression of bone matrix regulatory proteins in human atherosclerotic plaques." Arterioscler Thromb Vasc Biol **21**(12): 1998-2003.

Dubois, C., X. Liu, et al. (2010). "Differential effects of progenitor cell populations on left ventricular remodeling and myocardial neovascularization after myocardial infarction." J Am Coll Cardiol **55**(20): 2232-2243.

Duvall, C. L., D. Weiss, et al. (2008). "The role of osteopontin in recovery from hind limb ischemia." Arterioscler Thromb Vasc Biol **28**(2): 290-295.

Filipenko, N. R., S. Attwell, et al. (2005). "Integrin-linked kinase activity regulates Rac- and Cdc42-mediated actin cytoskeleton reorganization via alpha-PIX." Oncogene **24**(38): 5837-5849.

Gao, Y. A., R. Agnihotri, et al. (2004). "Expression and characterization of recombinant osteopontin peptides representing matrix metalloproteinase proteolytic fragments." Matrix Biol **23**(7): 457-466.

Gauer, S., A. Hartner, et al. (2003). "Differential regulation of osteopontin expression in the clipped and nonclipped kidney of two-kidney, one-clip hypertensive rats." Am J Hypertens **16**(3): 214-222.

Goncalves DaSilva, A., L. Liaw, et al. (2010). "Cleavage of osteopontin by matrix metalloproteinase-12 modulates experimental autoimmune encephalomyelitis disease in C57BL/6 mice." Am J Pathol **177**(3): 1448-1458.

Grassinger, J., D. N. Haylock, et al. (2009). "Thrombin-cleaved osteopontin regulates hemopoietic stem and progenitor cell functions through interactions with alpha9beta1 and alpha4beta1 integrins." Blood **114**(1): 49-59.

Green, P. M., S. B. Ludbrook, et al. (2001). "Structural elements of the osteopontin SVVYGLR motif important for the interaction with alpha(4) integrins." FEBS Lett **503**(1): 75-79.

Hakimzadeh, N., D. J. Stewart, et al. (2010). "The role of transglutaminase 2 and osteopontin in matrix protein supplemented microencapsulation of marrow stromal cells." Biomaterials **31**(35): 9256-9265.

Haylock, D. N. and S. K. Nilsson (2006). "Osteopontin: a bridge between bone and blood." Br J Haematol **134**(5): 467-474.

Hibbert, B., S. Olsen, et al. (2003). "Involvement of progenitor cells in vascular repair." Trends Cardiovasc Med **13**(8): 322-326.

Higashikawa, F., A. Eboshida, et al. (2007). "Enhanced biological activity of polymeric osteopontin." FEBS Lett **581**(14): 2697-2701.

Hu, Y., F. Davison, et al. (2003). "Endothelial replacement and angiogenesis in arteriosclerotic lesions of allografts are contributed by circulating progenitor cells." Circulation **108**(25): 3122-3127.

Huang, L., D. Hou, et al. (2007). "Acute myocardial infarction in swine rapidly and selectively releases highly proliferative endothelial colony forming cells (ECFCs) into circulation." Cell Transplant **16**(9): 887-897.

Hur, J., C. H. Yoon, et al. (2004). "Characterization of two types of endothelial progenitor cells and their different contributions to neovasculogenesis." Arterioscler Thromb Vasc Biol **24**(2): 288-293.

Infanger, M., M. Shakibaei, et al. (2005). "Intraluminal application of vascular endothelial growth factor enhances healing of microvascular anastomosis in a rat model." J Vasc Res **42**(3): 202-213.

Ingram, D. A., L. E. Mead, et al. (2005). "Vessel wall-derived endothelial cells rapidly proliferate because they contain a complete hierarchy of endothelial progenitor cells." Blood **105**(7): 2783-2786.

Ingram, D. A., L. E. Mead, et al. (2004). "Identification of a novel hierarchy of endothelial progenitor cells using human peripheral and umbilical cord blood." Blood **104**(9): 2752-2760.

Kalka, C., H. Masuda, et al. (2000). "Vascular endothelial growth factor(165) gene transfer augments circulating endothelial progenitor cells in human subjects." Circ Res **86**(12): 1198-1202.

Kalka, C., H. Masuda, et al. (2000). "Transplantation of ex vivo expanded endothelial progenitor cells for therapeutic neovascularization." Proc Natl Acad Sci U S A **97**(7): 3422-3427.

Kawabe, J., K. Yuhki, et al. (2011). "Prostaglandin I2 promotes recruitment of endothelial progenitor cells and limits vascular remodeling." Arterioscler Thromb Vasc Biol **30**(3): 464-470.

Kirton, J. P. and Q. Xu (2010). "Endothelial precursors in vascular repair." Microvasc Res **79**(3): 193-199.

Kitamura, M., K. Iwabuchi, et al. (2007). "Osteopontin aggravates experimental autoimmune uveoretinitis in mice." J Immunol **178**(10): 6567-6572.

Kolluru, G. K., S. Sinha, et al. (2010). "Shear stress promotes nitric oxide production in endothelial cells by sub-cellular delocalization of eNOS: A basis for shear stress mediated angiogenesis." Nitric Oxide **22**(4): 304-315.

Krasinski, K., I. Spyridopoulos, et al. (1997). "Estradiol accelerates functional endothelial recovery after arterial injury." Circulation **95**(7): 1768-1772.

Kroening, S. and M. Goppelt-Struebe (2010). "Analysis of matrix-dependent cell migration with a barrier migration assay." Sci Signal **3**(126): pl:1.

Kuliszewski, M. A., J. Kobulnik, et al. (2011). "Vascular Gene Transfer of SDF-1 Promotes Endothelial Progenitor Cell Engraftment and Enhances Angiogenesis in Ischemic Muscle." Mol Ther.

Leali, D., E. Moroni, et al. (2007). "Osteopontin overexpression inhibits in vitro re-endothelialization via integrin engagement." J Biol Chem **282**(27): 19676-19684.

Leen, L. L., C. Filipe, et al. (2008). "Estrogen-stimulated endothelial repair requires osteopontin." Arterioscler Thromb Vasc Biol **28**(12): 2131-2136.

Leone, A. M., M. Valgimigli, et al. (2009). "From bone marrow to the arterial wall: the ongoing tale of endothelial progenitor cells." Eur Heart J **30**(8): 890-899.

Liaw, L., M. Almeida, et al. (1994). "Osteopontin promotes vascular cell adhesion and spreading and is chemotactic for smooth muscle cells in vitro." Circ Res **74**(2): 214-224.

Liaw, L., V. Lindner, et al. (1995). "Osteopontin and beta 3 integrin are coordinately expressed in regenerating endothelium in vivo and stimulate Arg-Gly-Asp-dependent endothelial migration in vitro." Circ Res **77**(4): 665-672.

Lin, H. H., Y. H. Chen, et al. (2009). "After vascular injury, heme oxygenase-1/carbon monoxide enhances re-endothelialization via promoting mobilization of circulating endothelial progenitor cells." J Thromb Haemost **7**(8): 1401-1408.

Lin, Q., X. Ding, et al. (2010). "In situ endothelialization of intravascular stents coated with an anti-CD34 antibody functionalized heparin-collagen multilayer." Biomaterials **31**(14): 4017-4025.

Liu, L., G. Chen, et al. (2008). "Reduced foreign body reaction to implanted biomaterials by surface treatment with oriented osteopontin." J Biomater Sci Polym Ed **19**(6): 821-835.

Liu, S. Q., Z. L. Li, et al. (2011). "Transfusion of autologous late-outgrowth endothelial cells reduces arterial neointima formation after injury." Cardiovasc Res **90**(1): 171-181.

Malmstrom, J., B. Christensen, et al. (2010). "Osteopontin presentation affects cell adhesion-Influence of underlying surface chemistry and nanopatterning of osteopontin." J Biomed Mater Res A **95**(2): 518-530.

Masuda, H., C. Kalka, et al. (2000). "Endothelial progenitor cells for regeneration." Hum Cell **13**(4): 153-160.

Masuda, H., C. Kalka, et al. (2007). "Estrogen-mediated endothelial progenitor cell biology and kinetics for physiological postnatal vasculogenesis." Circ Res **101**(6): 598-606.

Mead, L. E., D. Prater, et al. (2008). "Isolation and characterization of endothelial progenitor cells from human blood." Curr Protoc Stem Cell Biol **Chapter 2**: Unit 2C 1.

Medina, R. J., C. L. O'Neill, et al. (2010). "Outgrowth endothelial cells: characterization and their potential for reversing ischemic retinopathy." Invest Ophthalmol Vis Sci **51**(11): 5906-5913.

Melero-Martin, J. M., Z. A. Khan, et al. (2007). "In vivo vasculogenic potential of human blood-derived endothelial progenitor cells." Blood **109**(11): 4761-4768.

Molin, D. G., N. M. van den Akker, et al. (2008). "Affirmative action of osteopontin on endothelial progenitors." Arterioscler Thromb Vasc Biol **28**(12): 2099-2100.

Murohara, T., T. Asahara, et al. (1998). "Nitric oxide synthase modulates angiogenesis in response to tissue ischemia." J Clin Invest **101**(11): 2567-2578.

Myers, D. L., K. J. Harmon, et al. (2003). "Alterations of arterial physiology in osteopontin-null mice." Arterioscler Thromb Vasc Biol **23**(6): 1021-1028.

Nilsson, S. K., H. M. Johnston, et al. (2005). "Osteopontin, a key component of the hematopoietic stem cell niche and regulator of primitive hematopoietic progenitor cells." Blood **106**(4): 1232-1239.

Nishimichi, N., F. Higashikawa, et al. (2009). "Polymeric osteopontin employs integrin alpha9beta1 as a receptor and attracts neutrophils by presenting a de novo binding site." J Biol Chem **284**(22): 14769-14776.

Oldberg, A., A. Franzen, et al. (1986). "Cloning and sequence analysis of rat bone sialoprotein (osteopontin) cDNA reveals an Arg-Gly-Asp cell-binding sequence." Proc Natl Acad Sci U S A **83**(23): 8819-8823.

Padfield, G. J., D. E. Newby, et al. (2010). "Understanding the role of endothelial progenitor cells in percutaneous coronary intervention." J Am Coll Cardiol **55**(15): 1553-1565.

Pagano, P. J. and M. J. Haurani (2006). "Vascular cell locomotion: osteopontin, NADPH oxidase, and matrix metalloproteinase-9." Circ Res **98**(12): 1453-1455.

Peloquin, J., J. Huynh, et al. (2011). "Indentation measurements of the subendothelial matrix in bovine carotid arteries." J Biomech **44**(5): 815-821.

Prater, D. N., J. Case, et al. (2007). "Working hypothesis to redefine endothelial progenitor cells." Leukemia **21**(6): 1141-1149.

Price, L. S., J. Leng, et al. (1998). "Activation of Rac and Cdc42 by integrins mediates cell spreading." Mol Biol Cell **9**(7): 1863-1871.

Rotundo, R., C. TM, et al. (2002). "TNF-alpha disruption of lung endothelial integrity: reduced integrin mediated adhesion to fibronectin." Am J Physiol Lung Cell Mol Physiol **282**(2): L316-329.

Scatena, M., L. Liaw, et al. (2007). "Osteopontin: a multifunctional molecule regulating chronic inflammation and vascular disease." Arterioscler Thromb Vasc Biol **27**(11): 2302-2309.

Schmidt-Lucke, C., F. Belgore, et al. (2005). "Soluble vascular endothelial growth factor, soluble VEGF receptor Flt-1 and endothelial function in healthy smokers." Int J Cardiol **100**(2): 207-212.

Schmidt-Lucke, C., L. Rossig, et al. (2005). "Reduced number of circulating endothelial progenitor cells predicts future cardiovascular events: proof of concept for the clinical importance of endogenous vascular repair." Circulation **111**(22): 2981-2987.

Senger, D. R., S. R. Ledbetter, et al. (1996). "Stimulation of endothelial cell migration by vascular permeability factor/vascular endothelial growth factor through cooperative mechanisms involving the alphavbeta3 integrin, osteopontin, and thrombin." Am J Pathol **149**(1): 293-305.

Shepherd, R. M., B. J. Capoccia, et al. (2006). "Angiogenic cells can be rapidly mobilized and efficiently harvested from the blood following treatment with AMD3100." Blood **108**(12): 3662-3667.

Singh, M., S. Ananthula, et al. (2007). "Osteopontin: a novel inflammatory mediator of cardiovascular disease." Front Biosci **12**: 214-221.

Smadja, D. M., I. Bieche, et al. (2008). "Bone morphogenetic proteins 2 and 4 are selectively expressed by late outgrowth endothelial progenitor cells and promote neoangiogenesis." Arterioscler Thromb Vasc Biol **28**(12): 2137-2143.

Smadja, D. M., I. Bieche, et al. (2005). "PAR-1 activation on human late endothelial progenitor cells enhances angiogenesis in vitro with upregulation of the SDF-1/CXCR4 system." Arterioscler Thromb Vasc Biol **25**(11): 2321-2327.

Smadja, D. M., P. Gaussem, et al. (2009). "Circulating endothelial cells: a new candidate biomarker of irreversible pulmonary hypertension secondary to congenital heart disease." Circulation **119**(3): 374-381.

Smadja, D. M., L. Mauge, et al. (2011). "Treprostinil increases the number and angiogenic potential of endothelial progenitor cells in children with pulmonary hypertension." Angiogenesis **14**(1): 17-27.

Smadja, D. M., L. Mauge, et al. (2010). "Distinct patterns of circulating endothelial cells in pulmonary hypertension." Eur Respir J **36**(6): 1284-1293.

Smadja, D. M., L. Mauge, et al. (2009). "Blood outgrowth endothelial cells from cord blood and peripheral blood: angiogenesis-related characteristics in vitro: a rebuttal." J Thromb Haemost **7**(3): 504-506; author reply 506-508.

Sodhi, C. P., S. A. Phadke, et al. (2001). "Hypoxia and high glucose cause exaggerated mesangial cell growth and collagen synthesis: role of osteopontin." Am J Physiol Renal Physiol **280**(4): F667-674.

Sodhi, C. P., S. A. Phadke, et al. (2001). "Hypoxia stimulates osteopontin expression and proliferation of cultured vascular smooth muscle cells: potentiation by high glucose." Diabetes **50**(6): 1482-1490.

Steinmetz, M., G. Nickenig, et al. (2010). "Endothelial-regenerating cells: an expanding universe." Hypertension **55**(3): 593-599.

Sumpio, B. E., J. T. Riley, et al. (2002). "Cells in focus: endothelial cell." Int J Biochem Cell Biol **34**(12): 1508-1512.

Suzuki, H., Y. Hasegawa, et al. (2010). "Mechanisms of osteopontin-induced stabilization of blood-brain barrier disruption after subarachnoid hemorrhage in rats." Stroke **41**(8): 1783-1790.

Takahashi, T., C. Kalka, et al. (1999). "Ischemia- and cytokine-induced mobilization of bone marrow-derived endothelial progenitor cells for neovascularization." Nat Med **5**(4): 434-438.

Timmermans, F., J. Plum, et al. (2009). "Endothelial progenitor cells: identity defined?" J Cell Mol Med **13**(1): 87-102.

Toutain, C. E., C. Filipe, et al. (2009). "Estrogen receptor alpha expression in both endothelium and hematopoietic cells is required for the accelerative effect of estradiol on reendothelialization." Arterioscler Thromb Vasc Biol **29**(10): 1543-1550.

Uede, T. (2011). "Osteopontin, intrinsic tissue regulator of intractable inflammatory diseases." Pathol Int **61**(5): 265-280.

Ueno H, K. H., Fukumoto S, Tanaka S, Shoji T, Shoji T, Emoto M, Tahara H, and K. R. Inaba M, Tabata T, Miyata T, Nishizawa Y (2011). "Advanced glycation end products, carotid atherosclerosis, and circulating endothelial progenitor cells in patients with end-stage renal disease." Metabolism **60**(4): 453-459.

Vaughan, E. E., A. Duffy, et al. (2009). Abstract 5443: Osteopontin Stimulates Secretion of Angiogenic Proteins in Endothelial Progenitor Cells, Circulation**:** S1093-a-.

Wang, S. H., S. J. Lin, et al. (2009). "Late outgrowth endothelial cells derived from Wharton jelly in human umbilical cord reduce neointimal formation after vascular injury: involvement of pigment epithelium-derived factor." Arterioscler Thromb Vasc Biol **29**(6): 816-822.

Werner, N., S. Kosiol, et al. (2005). "Circulating endothelial progenitor cells and cardiovascular outcomes." N Engl J Med **353**(10): 999-1007.

Werner, N., S. Wassmann, et al. (2006). "Circulating CD31+/annexin V+ apoptotic microparticles correlate with coronary endothelial function in patients with coronary artery disease." Arterioscler Thromb Vasc Biol **26**(1): 112-116.

White, F. J., J. W. Ross, et al. (2005). "Steroid regulation of cell specific secreted phosphoprotein 1 (osteopontin) expression in the pregnant porcine uterus." Biol Reprod **73**(6): 1294-1301.

Xu, Q. (2007). "Progenitor cells in vascular repair." Curr Opin Lipidol **18**(5): 534-539.

Yagisawa, T., F. Ito, et al. (2001). "The influence of sex hormones on renal osteopontin expression and urinary constituents in experimental urolithiasis." J Urol **166**(3): 1078-1082.

Yamahara, K. and H. Itoh (2009). "Potential use of endothelial progenitor cells for regeneration of the vasculature." Ther Adv Cardiovasc Dis **3**(1): 17-27.

Yin, Y., X. Zhao, et al. (2010). "SDF-1alpha involved in mobilization and recruitment of endothelial progenitor cells after arterial injury in mice." Cardiovasc Pathol **19**(4): 218-227.

Yoder, M. C., L. E. Mead, et al. (2007). "Redefining endothelial progenitor cells via clonal analysis and hematopoietic stem/progenitor cell principals." Blood **109**(5): 1801-1809.

Yu, M., Q. Liu, et al. (2011). "Effects of osteopontin on functional activity of late endothelial progenitor cells." J Cell Biochem **112**: 1730–1736.

Yu, X. Q., J. M. Fan, et al. (1999). "IL-1 up-regulates osteopontin expression in experimental crescentic glomerulonephritis in the rat." Am J Pathol **154**(3): 833-841.

Yu, X. Q., L. L. Wu, et al. (2000). "Osteopontin expression in progressive renal injury in remnant kidney: role of angiotensin II." Kidney Int **58**(4): 1469-1480.

Zhao, X., J. N. Johnson, et al. (2007). "Impairment of myocardial angiogenic response in the absence of osteopontin." Microcirculation **14**(3): 233-240.

6. Appendix

RNA microarray

The experiment started by coating 24 wells plate with 10 μM OPN, FN , or left uncoated as indicated in section 2.2. Confluent layer of L-EPCs incubated in 2% serum media one day before the assay. Next day, L-EPCs were detached using TrypLE^{TM}. After 10 minutes, TrypLE^{TM} was neutralized with 20% serum complete media and cells suspension was centrifuged at 220×g for 5 minutes. Then, supernatant was removed and cells re-suspended in 5 ml of PBS and re-centrifuged at 220×g for 5 minutes. After that, 100 μl of 5×10^4 cells/ ml in 2% serum media were incubated for 4 hours. Total RNA was isolated according to the manual instructions of RNAeas free mini kit from Qiagen. RNA samples were then sent to stem cell core at the Ottawa general hospital, in which samples quality were analyzed with bioanalyser (Eukariotic Total RNA nano test). Then, differential level between samples was evaluated by stem cell core at the Ottawa hospital research institute using Human gene 1ST array from Affymatrix. Data was analyzed with a trial version of ArrayStar. Data was collected by comparing fold of change in mRNA expression in L-EPCs seeded on OPN versus FN and uncoated plastic condition. Fold of change of more than 1.3 was selected ***Table 2***

Table 2: differential gene expression of L-EPC seeded on OPN coated surface vs FN coated surface and uncoated surface.

Probe Set ID	GO_molecular_function	gene_ assignment	Fold of change *vs* Uncoated	Fold of change *vs* FN
8168470	cytochrome-c oxidase activity	COX7B	3.17459178	0.885503054
8090509	GTPase activity	RAB7A	2.398720741	0.944409072
7951408	cysteine-type endopeptidase activity	CARD16	2.07693243	1.084605575
8005473	RNA binding translation activator activity	PAIP1	1.99894917	0.920683265
7934729	DNA binding	C1D	1.98241353	0.952177942
7934731	ligand-dependent nuclear receptor binding	C1D	1.968287706	1
8123819	protein binding	EEF1E1	1.955521822	0.997060061
8151532	transporter activity, fatty acid binding	FABP4	1.94021666	0.899678051
8039692	DNA binding, zinc ion binding.	ZNF814	1.923921347	0.887820899
8035847	DNA binding, metal ion binding	ZNF675	1.917049527	0.885375142
8165663	glycerol-3-phosphate O-acyltransferase activity	GPAM	1.903128386	0.874941945
8146934	lipopolysaccharide receptor activity	LY96	1.901854396	0.809095383
8053797	ion channel inhibitor activity	LOC400986	1.899524331	1.069717288
8065230	protein binding, hydrolase activity	RBBP9	1.893262029	0.856676042
8095744	cytokine activity, growth factor activity	AREG	1.890295744	1
8145660	transferase activity	DCTN6	1.883037329	0.980938017
7896750	glycerol-3-phosphate O-acyltransferase activity	GPAM	1.842003942	0.876482844
7918284	RNA polymerase II transcription factor activity	TAF13	1.830263972	0.89294374
7971550	transcription cofactor activity	MED4	1.813011885	0.965839505
7979416	protein binding	TIMM9	1.804605007	0.766651034
8052698	DNA binding	C1D	1.796396852	1.038336515
8063453	unfolded protein binding	PFDN4	1.789465308	0.918238759
8021635	serine-type endopeptidase activity	SERPINB2	1.787751436	0.642000914
8176276	nucleotide binding	ATRX	1.778921962	0.833004057
8012000	endoribonuclease activity	RNASEK	1.766265273	1
8175288	structural molecule activity	MOSPD1	1.759445906	0.882876456
7926889	lysozyme activity	LYZL1	1.733551025	1
8026339	RNA binding	SNRPG	1.721947789	0.895859122
8105852	structural constituent of ribosome	MRPS36	1.686535478	1
8097058	protein binding	CEP170L	1.686370969	0.982579529
7978653	GTPase activator activity activator	RALGAPA1	1.685031056	1.035238028
8101489	protein binding	FAM175A	1.678483725	0.894480169
7965867	melanin-concentrating hormone activity	PMCH	1.676422834	0.950407445
8142878		CDC26	1.676195145	1
7918008	protein binding dihydrolipoyllysine-residue (2-methylpropanoyl)transferase activity	DBT	1.674892664	0.911153853
7958031	DNA binding	C12orf48	1.671727538	0.797404528
8107458	protein binding	COMMD10	1.669425011	0.876739264
8035773	DNA binding	ZNF506	1.668899179	0.967271328
8085754	protein binding	SGOL1	1.667574286	0.949883938
7932964	DNA binding	C1D	1.660816431	1.01367569
8030978	DNA binding	ZNF845	1.65900588	0.814288497
8113356	glycerol-3-phosphate O-acyltransferase activity	GPAM	1.65480876	1
8027348	DNA binding	ZNF730	1.653000474	0.764915764
8066528	GPI-anchor transamidase activity	PIGT	1.651505828	1

7965681	protein binding	IKBIP	1.650595069	0.823951602
8086451	protein binding	HIGD1A	1.640914321	0.992533803
7961514	extracellular matrix structural constituent	MGP	1.639819741	1
7907156	cytokine activity	XCL1	1.635858178	1.116815925
7927658	nucleotide binding	UBE2D1	1.633623004	0.849122882
8159004	RNA binding	SNORD24, RPL7A	1.633188367	1.014935851
8113050	calcium ion binding	CETN3	1.623782277	1.182740569
8027254	sequence-specific DNA binding transcription factor activity	ZNF90	1.619315982	1.019986629
8137464	phosphoserine phosphatase activity	PSPH	1.609623432	0.993376374
8092067	structural constituent of ribosome	RPL22L1	1.604588985	0.82011342
8119595	structural constituent of ribosome	RPL7L1	1.603556752	0.895212173
8096938	nucleotide binding	LARP7	1.597177029	1
7966315	actin binding	ARPC3	1.596993923	0.99556303
7951034	DNA binding	SNORA8, TAF1D	1.594125032	0.988414943
8054217	protein binding	TXNDC9	1.586030006	0.840310693
7957540	structural constituent of ribosome	MRPL42	1.585658908	0.846335292
8005157	N-acetylglucosaminylphosphatidylinositol deacetylase activity	PIGL	1.58328712	1
8121510	protein binding	RPF2, BXDC1	1.581591368	0.896993995
7995258	DNA binding	ZNF267	1.578985572	1
8086216	acetyl-CoA C-acyltransferase activity	ACAA1	1.576412559	1.654116035
8017262	nucleotide binding	BRIP1	1.575889707	0.937001765
8027272	DNA binding	ZNF85	1.574656725	1
8135488	protein binding	LRRN3	1.573765993	1
7918467	protein binding	C1orf103	1.56966114	0.952844441
8084035	sequence-specific DNA binding transcription factor activity	ZNF639	1.568750381	0.873119831
7925691	DNA binding GO:0003677, zinc ion binding	ZNF124	1.567995548	0.916425347
7968658	3'-5'-exoribonuclease activity	EXOSC8	1.567315221	0.797044396
7947248	nucleotide binding	KIF18A	1.566538453	0.933701873
8095736	cytokine activity	AREG	1.559753299	1
8096109	structural constituent of ribosome	MRPS18C, FAM175A	1.558849812	0.838914096
8092321	molecular_function	DCUN1D1	1.55753088	0.83068651
8160587	NADH dehydrogenase (ubiquinone) activity	NDUFB6	1.55727458	0.884221435
8051993	ethanolaminephosphotransferase activity	PIGF,	1.556971431	1
8097529		ELMOD2	1.552108288	0.990383506
8117225	protein binding	GMNN	1.549353361	0.85770762
8162624	antioxidant activity	C9orf21	1.54868722	0.904004276
7958147	damaged DNA binding	TDG	1.548686743	1
8105908	structural molecule activity	OCLN	1.546998978	0.822636843
8104825	molecular_function	BRIX1, RAD1, BXDC2	1.546285868	0.918735743
7999360	RNA binding	RPL21	1.544732928	0.937485337
7953733	DNA binding	ZNF705A	1.542142987	1
8059852		MSL3L2	1.541279316	0.762320697
8160332	protein binding	MLLT3	1.540798545	0.92806685

8122818	protein binding	C6orf211	1.539628625	0.932950675
8151909	ubiquinol-cytochrome-c reductase activity	UQCRB	1.539582372	1
8054437	protein binding	ANAPC1	1.538476944	0.95079267
8127743	DNA binding	HMGN3	1.536251426	0.920767903
8132843	molecular_function	HAUS6	1.534062028	0.973552048
7924144	RNA binding	RPL21P28, RPL21	1.530378699	0.95346415
8114152	protein binding	SKP1	1.530004025	0.971456885
8109830	protein binding	CCDC99	1.529589415	0.85714221
8171418	protein binding	PIGA	1.529188037	0.881161094
8131803	cytokine activity	IL6	1.521372437	0.82315737
8174610	protein binding	LRCH2	1.519080758	0.945217848
8112331	structural molecule activity	ISCA1	1.518862367	1
8124459	DNA binding	ZNF322A	1.518753886	0.8779549
7979698	protein binding	ATP6V1D	1.51806736	0.897112548
7979931	RNA polymerase II transcription factor activity	MED6	1.517569661	0.94633019
7974603	threonine-type endopeptidase activity	PSMA3	1.517460346	0.814779222
8088526	RNA binding	THOC7	1.517454386	0.879466295
7970546	calcium ion binding	EFHA1	1.51621151	0.900051057
7902400	prenyltransferase activity	SNORD45B , RABGGTB	1.51418674	0.927314401
8112182	DNA binding	MIER3	1.510889769	0.899018168
8081055	protein binding	CHMP2B	1.510679603	0.892856359
8178322	protein binding	SUMO2	1.508342624	0.934584618
7943162	protein binding	C11orf54	1.506592751	1
8100808	estrone sulfotransferase activity	SULT1E1	1.50637567	0.909648955
8101131	chemokine activity	CXCL11	1.505903721	0.851427078
7983663	cysteine-type endopeptidase activity	USP8	1.504192591	0.971911013
8105348	glutathione peroxidase activity	GPX8	1.502216101	0.907061934
8012949	molecular_function	CDRT1, FBXW10	1.501021981	1
8047288	protein binding	SGOL2	1.500376701	1
8051226	methyltransferase activity	TRMT61B, SPDYA	1.500376701	0.820584357
8053036	protein kinase binding	TPRKB	1.500130773	0.948824048
8094625	molecular_function	KLHL5	1.470062733	0.995670378
7927710	nucleotide binding	CDK1, CDC2	1.469304919	0.850823045
7938880	RNA polymerase II transcription factor activity	HTATIP2	1.46582222	0.950256407
8072113	nucleic acid binding	SRRD, TFIP11	1.463917494	0.931949437
8056693	protein kinase activity	FASTKD1	1.449501514	0.824490547
8177222	signal transducer activity	CD24	1.449064612	0.779769659
7917255	protein binding	SSX2IP	1.443304777	0.949681163
8095422	protein binding	STATH	1.437607884	1.101505995
8057034	double-stranded RNA binding	PRKRA	1.432112336	0.998326063
8089314	DNA binding	IFT57	1.426626921	0.853534579
7974587	protein binding	ACTR10	1.424034476	0.830628872
7918902	protein binding	CD58	1.414717555	1
7933047	protein binding	CUL2	1.411144018	0.934211195
7964460	DNA binding	DDIT3	1.409113884	1
8096808	cysteine-type endopeptidase activity	CCDC109B	1.402646542	1
7908351	lysophospholipase activity	PLA2G4A	1.402089	0.9160344

7954729	guanyl-nucleotide exchange factor activity	FGD4	1.399283051	0.932236195
8001410	protein binding	AKTIP	1.379916072	0.980147839
8078918	structural constituent of ribosome	SNORA62, RPSA	1.379119992	0.997948945
7927669	sequence-specific DNA binding transcription factor activity	TFAM	1.378928065	0.882369399
7988031	RNA binding	RPS3A	1.375228167	0.952197492
7954029	protein kinase inhibitor activity	CDKN1B	1.364537835	1
8110920	protein kinase activity	FASTKD3	1.364138365	0.812365294
8112980	integrin binding	EDIL3	1.36029911	0.866104543
7969835	GTP binding	PCCA	1.356602192	0.981399357
8134079	GTP binding	GTPBP10	1.353685856	0.995484114
8095680	interleukin-8 receptor binding	IL8	1.351857662	0.880959988
7900201	protein binding	UTP11L	1.348900676	0.864164114
7906041	protein binding	DAP3	1.346299529	1
7943605	acetyl-CoA C-acetyltransferase activity	ACAT1	1.345975637	0.905015469
8047443	nucleotide binding	STRADB	1.345025301	1
8120102	structural constituent of cytoskeleton	CD2AP	1.344922185	0.881181777
7990818	protein binding	BCL2A1	1.343356967	0.811368167
8151967	nucleotide binding	STK3	1.340977073	0.938800633
8051501	nucleotide binding	EIF2AK2	1.326277733	0.959284723
8135625	actin binding	CAPZA2	1.325395226	0.898346841
8140556	catalytic activity	HGF	1.318281293	1
8091941	protein binding	PDCD10	1.315310001	0.867588282
8147206	nucleotide binding	RIPK2	1.313508034	0.852971733
7989493	structural constituent of ribosome	RPS27L	1.307972312	1
8141050	RNA binding	RPS3A	1.302728534	0.939847529
8050176	protein binding	ITGB1BP1	1.301224113	0.855838656
7951217	metalloendopeptidase activity	MMP7	1.196814179	1
7951259	metalloendopeptidase activity	MMP10	1.167395353	0.992312133
8151684	metalloendopeptidase activity	MMP16	1.145471454	1
8085350		C3orf31	1.085756779	1
7951271	metalloendopeptidase activity	MMP1	1.064522266	0.96957624
7956038	metalloendopeptidase activity	MMP19	1.03548646	1.01765132
7995681	metalloendopeptidase activity	MMP2	0.985361159	1.016089439
7959946	metalloendopeptidase activity	MMP17	0.984115541	1
7951309	metalloendopeptidase activity	MMP13	0.977334082	1
7936928	metalloendopeptidase activity	MMP21	0.958001196	1.111397386
8063115	metalloendopeptidase activity	MMP9	0.942808807	1.041861534
8071758	metalloendopeptidase activity	MMP11	0.942705035	1
7962918	signal transducer activity	WNT10B	0.767191768	1.037365675
7977371		PACS2	0.765987456	1
8070757	structural molecule activity	C21orf29	0.76468724	1.012754321
8159096	catalytic activity	DBH	0.764675379	1
8082473	protein binding	GP9	0.762693167	1.073711038
7905571	signal transducer activity	S100A9	0.761511087	1.004018188
8049534	DNA binding	LRRFIP1	0.761265695	1.37718451
8009517	RNA polymerase II transcription factor activity	SOX9	0.759738684	1.003461242
7995161	receptor activity	ITGAD	0.759070814	1.090072513
7902038	nucleotide binding	AK3L1	0.758033872	1.006718397
8134907	erythropoietin receptor binding	EPO	0.758018076	1.130378604
7956120	nucleotide binding	ERBB3	0.756510556	1.011847734
8137183	protein binding	SSPO	0.755503058	1

8165107	protein binding	CARD9	0.755503058	1.100081444
7953012	signal transducer activity	WNT5B	0.755069196	0.983430743
7897860	transmembrane receptor activity	TNFRSF8	0.754845381	1.208286405
7934719	protein binding	SFTPD	0.752143502	1.301539779
7993848		OTOA	0.752071917	1
8046922	integrin binding	COL3A1	0.75109911	1
8178712	integrin binding	TNXB	0.748070598	1.056788087
8179935	integrin binding	TNXB	0.748070598	1.056788087
8030563	protein binding	SIGLEC16	0.747713923	1
7923700	receptor activity	LRRN2	0.746307075	1.026041031
7960253	protein binding	NINJ2	0.743843257	1
8082368	protein binding	PODXL2	0.741031587	1.006625533
8029530	beta-amyloid binding	APOE	0.737219393	1.123425484
8049536	DNA binding	LRRFIP1	0.735082865	1.176306844
8166899	molecular_function	NYX	0.734625518	1.139798284
7947563	DNA binding	ALX4	0.732715428	1.079235435
7914232	actin binding	TMEM200B, EPB41	0.732211828	1.033161879
7897006	metalloendopeptidase activity	MMP23B	0.730425596	1.244291663
8037872	protein binding	BBC3	0.729449451	1
8007895	signal transducer activity	WNT9B	0.726284444	1.088310242
8087852	transmembrane receptor activity	TLR9, TWF2	0.72391808	1.277678847
8049528	DNA binding	LRRFIP1	0.723091662	1.115692258
8033825	extracellular matrix structural constituent	COL5A3	0.719958305	1.119650722
7971905	calcium ion binding	PCDH20	0.717758656	1
8108703	calcium ion binding	PCDHB6	0.713232696	1
8168264	protein binding	NLGN3	0.712281525	1
7940851	receptor signaling protein activity	FLRT1	0.710999906	1.042942286
7935528	protein binding	SFRP5	0.710653365	1.022027493
8099279	actin binding	ABLIM2	0.706357419	1
7985522	peptidase activity	ADAMTSL3	0.70576936	1
7997880	calcium ion binding	CDH15	0.705085516	1.103658915
8049737	serine-pyruvate transaminase activity	AGXT	0.695626855	1.055242658
7920155	calcium ion binding	HRNR, RPTN	0.69480288	1.071736574
7963142	protein binding	FAIM2	0.694357514	1
8135099	protein binding	EMID2	0.692531943	1.089819431
7898184	serine-type endopeptidase activity	CELA2B	0.691942573	1.1851542
7921155	nucleotide binding	INSRR	0.691301167	1
8173493	receptor activity	CXCR3	0.68871516	1
8125289	molecular_function	TNXA	0.687601566	1.189133644
8049487	actin binding	MLPH	0.686711311	1.031408072
7981730	antigen binding	IGLJ3	0.666664541	1
8007826	aspartic-type endopeptidase activity	IMP5	0.666603029	1.22688663
7981783	receptor activity	OR4N4	0.666433215	0.641103268
8159531	binding	LCNL1	0.665854394	1.044461131
8018445	nucleic acid binding	UNK	0.665854394	1
7952309		BLID	0.664996862	0.77112633
7906613	receptor activity	SLAMF7	0.664756	0.920261621
7981740	antigen binding	IGHA1	0.664391816	1.222804308
8071274	transmembrane receptor activity	GP1BB	0.663233161	1.141446829
8172026			0.663012207	1
8033043	fucosyltransferase activity	FUT6	0.662302136	1

7923534	protein binding	MYBPH	0.662252009	1.133087754
8179309	protein binding	LY6G6D	0.661563993	1.12004602
8178070	protein binding	LY6G6D	0.661563993	1.12004602
8148821	DNA binding	SCXA, SCXB	0.65984273	1
8148796	DNA binding	SCXA, SCXB	0.65984273	1
7920185		LCE3D	0.659084916	1.091196656
7912520	receptor binding	NPPB	0.656972408	1.059095621
8015366	structural constituent of cytoskeleton	KRT14	0.649004281	1.007747412
7967322	receptor activity	GPR109B	0.647147238	0.974921584
8049538	DNA binding	LRRFIP1	0.646573067	1.216079831
8167573	molecular_function	GAGE1	0.646033943	1.282661796
8159259	transporter activity	OBP2A	0.645968616	1
8036686	protein binding	FBXO17	0.638536036	1.078798175
8012951	molecular_function	CDRT1, FBXW10, TRIM16	0.627597213	0.626832247
8165295	binding	LCN8	0.627075553	1.334084034
7918416	sequence-specific	ALX3	0.624189258	1.137809753
7939657	nucleotide binding	DGKZ	0.621410787	0.922096074
8007127	protein binding	KRTAP9-3	0.610305429	0.866030633
8006367	serine-type endopeptidase activity	RHBDL3	0.594113648	0.868226647
8006602	receptor signaling protein tyrosine kinase activity	CCL4	0.574356019	1
8130598	molecular_function	LPAL2	0.553452015	0.79496479
8180022	MHC class II receptor activity	HLA-DQB1	0.546717227	0.985491633
8178826	MHC class II receptor activity	HLA-DQB1	0.546717227	0.985491633
7981781	receptor activity	OR4M2	0.545998037	0.644068241
7911233	receptor activity	OR2T8	0.525538683	1
7939988	receptor activity	OR5M3	0.504260004	1

Selected genes

Probe Set ID	**GO molecular function**	**Fold change *vs* uncoated**	**Fold change *vs* FN**	**Gene assignment**	**Level of expression out of 12**
7923978	Stem cell markers	0.98	1	CD34	11.23414
7939341	Receptor activity	1	0.86	CD44	9.95726
8055465	Chemokine reseptor	1.04	1.01	CXCR4	7.93046
7960464	Endothelium marker	0.91	1	VWF	10.4888
8017599	Adhesion molecule	1	1	PECAM1	11.64607
8100393	Vascular endothelial growth factor receptor	1	1	KDR	10.73056
8050176	β1 integrin binding protein	1.30	0.85	ITGB1BP1	7.63387

Western blot data:

	Bands intensities	**% Percentages *vs***	**Average**	**Standarad**

BIOLOGICAL EFFECTS OF OPN ON EPCs

		uncoated condition		**error**
Unblocked/ OPN	0.255915842	3.105952645	***3.060***	***0.516***
CD44/OPN	0.120346233	1.46059618	***2.174***	***0.611***
B1integrin/OPN	0.12074503	1.465436225	***2.066***	***0.412***
Uncoated/ unblocked	0.082395281	1	***1***	***0***
Unblocked/ OPN	2.783987726	3.93144261		
CD44/OPN	2.40109087	3.390730091		
B1integrin/OPN	2.022720873	2.856410233		
Uncoated/ unblocked	0.708133884	1		
Unblocked/ OPN	1.517726206	2.143275784		
CD44/OPN	1.183658354	1.671517746		
B1integrin/OPN	1.330130772	1.878360578		
Unblocked/ OPN	0.708133884	1		

L-EPCs migration to cell free area

	Coatings	0	1	10	100
	OPN	34	44	50	59
Trile One		28	29	57	86
	FN	21	100	109	112
		34	107	96	130
	FN	34	98	118	182
Trile Two		28	76	110	188
	OPN	21	40	45	69
		34	38	48	66
Average	OPN	29.25	37.75	50	70
	FN	29.25	95.25	108.25	153
Standard Error	OPN	1.54616461	1.586072193	1.274754878	2.865018906
	FN	1.54616461	3.350217655	2.27646473	9.438396757

Receptor Blocking

	OPN	OPN/ CD44	OPN/B1	OPN/ CD44, β1	ISOTYPE
A) 1:	99	102	93	69	139
	105	86	65	78	99

	128	90	88	71	138
	169	87	96	63	101
A) 2:	117	94	87	50	109
	152	84	75	64	91
	145	81	93	67	107
	138	124	86	69	95
B) 1:	28	24	20	14	
	161	29	20	12	
	27	15	13	14	
	103	30	18	10	
B) 2:	53	14	16	24	
	28	27	31	14	
	51	19	14	20	
	59	14	16	11	
C) 1:	150	37	28	42	
	141	67	58	38	
	178	81	75	49	
	150	36	90	59	
C) 2:	180	66	93	39	
	187	68	63	42	
	217	102	71	51	
	155	93	84	52	
A) 1:	125.25	91.25	85.5	70.25	119.25
A) 2:	138	95.75	85.25	62.5	100.5
B) 1:	79.75	24.5	17.75	12.5	
B) 2:	47.75	18.5	19.25	17.25	
C) 1:	154.75	55.25	62.75	47	
C) 2:	184.75	82.25	77.75	46	
A)	131.625	93.5	85.375	66.375	109.875
B)	63.75	21.5	18.5	14.875	
C)	169.75	68.75	70.25	46.5	
percentage vs OPN	100	71.03	64.86	50.42	83.47578348
	100	33.72	29.01	23.33	
	100	40.50	41.38	27.39	
Average	100	48.42	45.08	33.71	83.47578348
Standard Error	0	11.47	10.51	8.43	0

Flow experiment (OPN/ Flow; OPN/ Uncoated; OPN/ Static)

OPN/ Flow

	FLOW/OPN				
Res (ohm)	Res. (ohm)	Res. (ohm)	Res. (ohm)		
Average	Average	Average	Average	Average	Standard Error
3186.1	2338.5625	2223.15	2025.285714	2443.274554	255.9172631
3450.2	2384.15	2213.45	2222.142857	2567.485714	296.8444416
3460.1	2398.9875	2219.55	2347.857143	2606.623661	286.9844314
3485.35	2438.8625	2228.4375	2452.142857	2651.198214	282.7315149
3568.85	2459.575	2250.6875	2491.714286	2692.706696	296.8945373
3690.5	2531.55	2013.075	2753.428571	2747.138393	350.6301599
3790.6	2564.75	1582.3	2875.142857	2703.198214	455.3010285
3836.15	2613.9125	1698.9	2801	2737.490625	438.2757791
3906.9	2631.05	1798.9625	2692.857143	2757.442411	433.981834
3958.7	2683.9125	1903.475	2902.857143	2862.236161	423.7634272
3964.85	2712.725	2022.8875	2870.428571	2892.722768	401.9708139
4011.4	2767.3875	2140.7875	2765.857143	2921.358036	392.1489193
4007.9	2832.375	2271.5	2923.571429	3008.836607	362.8821876
4063.05	3003.2375	2430.8	2931	3107.021875	343.1497119
4046.9	3077.925	2633.6125	2940	3174.609375	305.226416
4137.9	3195.0875	2858.6	2895.714286	3271.825446	298.3550345
4148.15	3224.5125	3071.25	3013.428571	3364.335268	265.039372
4358.25	3294.7875	3279.725	2995.142857	3481.976339	300.1121504
4446.3	3351.5625	3579.675	3163.857143	3635.348661	283.3696743
4632.45	3371.4875	3879.55	3241.714286	3781.300446	315.3316261
4707.2	3418.125	4156.9625	3302.285714	3896.143304	330.0262556
4726.35	3477.4	4487.425	3176.857143	3967.008036	377.655983
5007	3572.8875	4833.425	3197.571429	4152.720982	451.0790892
5092.9	3618.4875	5210	3382.571429	4325.989732	479.6025278
5204.3	3679.8125	5598.4	3423.428571	4476.485268	542.5267164
5402.2	3813.45	6036.6125	3443.857143	4674.029911	621.877923
5670.45	3881.625	6828.7875	3323.142857	4926.001339	808.0158947
5875.75	3922.1125	7184.4375	3451.571429	5108.467857	868.4812727
5953.1	4040.3625	7589.625	3383	5241.521875	953.800255
5899.3	4082.025	7991.8875	3249.142857	5305.588839	1052.567179
6033.35	4046.4875	8342	3312	5433.459375	1127.081711
6073.25	4188.95	8637.45	3383.285714	5570.733929	1167.316238
6041.5	4281.9125	8914.575	3498.428571	5684.104018	1200.936887
6147.05	4325.6	9291.0875	3311.714286	5768.862946	1312.430275
6413.6	4437.5625	9615.725	3162	5907.221875	1405.511652
6576.05	4462.625	9687.8125	2996	5930.621875	1452.012375
6602.75	4564.275	9838.425	3004.857143	6002.576786	1475.606499
6735.55	4632.8625	9930.0875	3048	6086.625	1487.166628
6763.8	4787.1875	10134.1375	3005.142857	6172.566964	1527.401097
6696.25	4885.9125	10461.0875	2842	6221.3125	1617.722262
6922.15	4919.1	10700.8125	3166.285714	6427.087054	1618.040658
7096.9	4897.275	10973.5125	3439.142857	6601.707589	1639.735747
7206.6	5049.8875	10949.7625	3492.142857	6674.598214	1615.749634
7221.6	5142.9375	11281.35	3547	6798.221875	1673.023632
7485.7	5241.375	11248.125	3608.714286	6895.978571	1654.10523
7552.35	5390.0375	11320.3625	3339.428571	6900.544643	1705.94108
7615.2	5348.2875	11524.5875	3378.714286	6966.697321	1748.518211
7780.35	5541.4125	11715.825	3575	7153.146875	1746.716877
7688.85	5566.0375	11572.3875	3556.571429	7095.961607	1714.104626
7631.55	5639.1625	11812.875	3462.285714	7136.468304	1776.12471

7467.35	5701.4625	12104.825	3626.142857	7224.945089	1806.109188
7597.85	5716.475	12142.8125	3797.428571	7313.641518	1786.905174
7858.7	5790.1125	12246.45	4047	7485.565625	1767.850487
7895.8	5763.4	12263.5375	3933.428571	7464.041518	1793.018554
7857.65	5728.2375	12493.3125	3941.571429	7505.192857	1845.321373
7936.95	5910.075	12327.6	4068	7560.65625	1774.551959
8082.55	6108.7	12422.9875	4152.142857	7691.595089	1769.467878
8059.25	6190.0875	12156.5875	4141.571429	7636.874107	1705.787766
7951.5	6179.475	12192.0875	3992.714286	7578.944196	1737.801484
7804.1	6256.3625	12298.275	4118.428571	7619.291518	1733.028599
7722.45	6302.8625	12196.9	3960.285714	7545.624554	1733.607574
7526.15	6285.8125	12340.9375	3896.571429	7512.367857	1777.022242
7519.35	6403.4875	12317.975	3988.571429	7557.345982	1749.585035
7701.75	6473	12332.7	4313.285714	7705.183929	1694.037768
7711.7	6585.625	12393.7125	4392.142857	7770.795089	1688.065378
7351.7	6507.4875	12524.7125	4393.714286	7694.403571	1726.090226
7319.85	6500.35	12721.3375	4435	7744.134375	1766.586588
7160.95	6584.6	12985.425	4328.571429	7764.886607	1844.363011
7193.8	6655.725	12999.0375	4416.571429	7816.283482	1829.238524
7370.9	6777.7875	12990.325	4423.714286	7890.681696	1815.097136
7471.75	6919.5375	13121.0125	4337.285714	7962.396429	1850.248545
7491.7	6879.7125	12959.375	4217.285714	7887.018304	1834.091085
7462.4	6964.225	13337.0625	4318.428571	8020.529018	1901.717692
7297.5	6995.9125	13596.45	4214	8025.965625	1982.276673
6967.5	6985.1625	13857.575	4231.285714	8010.380804	2053.653505
6938.7	7069.225	13870.4125	4170.857143	8012.298661	2063.899479
7020.3	7352.7875	13747.3375	4095.142857	8053.891964	2034.020575
7024.5	7457.8375	13664.6	4335.142857	8120.520089	1972.864058
7027.75	7565.5	13658.225	4462	8178.36875	1948.070687
6861.4	7590.3625	13314.275	4622.428571	8097.116518	1850.134993
6980.7	7600.25	13649.6875	4670.428571	8225.266518	1914.871782
7103.45	7613.9375	13836.775	4588.714286	8285.719196	1964.924022
7083.15	7732.8375	13977.6875	4586.571429	8345.061607	1996.245687
7186.25	7762.6625	14208.325	4664.857143	8455.523661	2032.137383
7288.6	7705.8875	14187.875	4698.142857	8470.126339	2018.674785
7293.7	7732.8125	14270.6375	4822	8529.7875	2018.004962
7359.35	7749.7625	14288.5375	4851.142857	8562.198214	2013.905598
7659	7867.1	14432.475	4679.142857	8659.429464	2057.494053
7605.95	7990.225	14739.5125	4751.428571	8771.779018	2116.345998
7517.2	8090.8	14985.7	4580.285714	8793.496429	2202.597793
7422.9	8276.7375	12926.575	4420.428571	8261.660268	1761.16052
7479.6	8425.0375	12469.4375	4509.142857	8220.804464	1643.634432
7509.75	8442.9375	13129.9375	4562.428571	8411.263393	1777.009296
7503.05	8583.225	13805.4125	4889.428571	8695.279018	1871.53965
7517.7	8690.6125	14239.3375	4669	8779.1625	2006.366441
7644.45	8765.9125	14636.05	4674.857143	8930.317411	2088.556328
7479.3	8769.6125	14372.8	4510.142857	8782.963839	2065.651332
7538.3	8632.6875	14373.5875	4544.714286	8772.322321	2057.286852
7498.5	8614.75	14258.0875	4787.142857	8789.620089	1992.099614
7264.85	8532.7	14288.2125	4761.714286	8711.869196	2017.120361
7330.95	8493.9	14406.925	5004.142857	8808.979464	2002.032759
7533.4	8823.6375	14358.975	5191	8976.753125	1945.228172
7939.9	8764.9625	14248.1	5131.142857	9021.026339	1908.050825
7980.65	8685.3125	14116.8875	5016.142857	8949.748214	1896.963738
7854.8	8768.1375	14259.9125	4913.714286	8949.141071	1951.90734

7797.85	8958.125	14269.825	4831.285714	8964.271429	1970.428176
8031.55	9089.1875	14330.5	4673.571429	9031.202232	2001.54461
7898.05	9124.8375	14547.35	4721	9072.809375	2047.18519
8071.8	9084.9	14717.8625	5235.428571	9277.497768	1988.020222
8456.5	8942.2625	14706.25	5315.428571	9355.110268	1956.435286
8129.7	8997.3125	14896.05	5583.428571	9401.622768	1969.530228
8198.9	9099.8375	15147.75	5668.285714	9528.693304	2008.913729
8720.65	9156.9	15204.075	5700.285714	9695.477679	1990.53088
8636.75	9212.55	15152.1625	5683.428571	9671.222768	1983.761526
8784.1	9063.475	15549.4125	5877.428571	9818.604018	2041.556762
8453.5	9050.4125	15539.6375	5994.571429	9759.530357	2037.014109
8456.9	9279.6875	15504.25	6131.428571	9843.066518	2001.335142
8587.85	9132.475	15658.9125	6259.714286	9909.737946	2015.093178
8753.35	9214.8375	15885.3125	6246	10024.875	2059.481337
8471.55	9302.025	15909.6	6332.285714	10003.86518	2065.566286
8501.85	9483.5	15847.0375	6463.142857	10073.88259	2024.569853
8865.85	9554.25	16041.8	6447.142857	10227.26071	2049.482469
8779.45	9460.8875	16072.5875	6360.285714	10168.30268	2077.476844
8819.9	9548.65	16250.4125	6393.142857	10253.02634	2109.844749
9012.3	9447.325	16048.2	6110.142857	10154.49196	2099.548398
9208.35	9656.0125	16240.2	6075.714286	10295.0692	2135.745151
9165.15	9601.925	16180.9625	6171.142857	10279.79509	2109.635464
8919.85	9673.1625	16295.95	6359.428571	10312.09777	2116.929251
8650.95	9572.125	16716.6625	6393.857143	10333.39866	2230.026452
8405	9443.1375	16584.125	6445.142857	10219.35134	2210.757263
8722.2	9282.5375	16764.675	6465.714286	10308.7817	2236.406047
8898	9295.95	16651.1875	6473.571429	10329.67723	2197.523904
8964.35	9747.475	16678.6125	6571.571429	10490.50223	2170.483
8902.4	9839.15	16771.7125	6603.714286	10529.2442	2189.007531
9120.65	9651.9375	16734.4375	6562.857143	10517.47054	2179.256379
9458	9619.85	16823.5875	6373.285714	10568.6808	2214.706329
9479.9	9476.2125	16719.95	6246.285714	10480.58705	2214.894667
9436.05	9588.3125	16676.225	6037.714286	10434.57545	2236.138622
9173.3	9581.975	16348.5	5748.857143	10213.15804	2218.33459
8961.85	9623.2125	16731.65	5665.428571	10245.53527	2328.844405
8810.75	9269.5125	16488.825	5625.142857	10048.55759	2294.608193
9057.85	9486.5125	16573.7375	5429.857143	10136.98929	2330.530738
9173.65	9593.8875	17437.125	5457.571429	10415.55848	2518.291615
9369.15	9572.7875	17444.125	5543	10482.26563	2498.83319
9667.8	9587.025	17297.0625	5655	10551.72188	2435.663209
9639.8	9416.775	17038.3	5495.571429	10397.61161	2409.44425
9546.95	9548.9875	14874.15	5489.571429	9864.914732	1924.33925
9342.85	10007.175	12119.0625	5580.285714	9262.343304	1362.584806
9515.75	10221.25	13147.9125	5486.714286	9592.906696	1578.492182
9480.75	10209.425	14731.7375	5553.714286	9993.906696	1881.314419
9359.8	10260.7875	15296.0625	5582.571429	10124.80536	1999.531483
9082.45	10134.1125	15298.4625	5633.714286	10037.18482	1999.843934
9207.85	10060.55	15701.0375	5607.285714	10144.1808	2088.575728
9241.05	9924.2125	15803.975	5373.714286	10085.73795	2153.311213
9418.6	9934.3	13893.15	5503	9687.2625	1715.875612
9607.6	10147.0875	11100.1125	5710.285714	9141.271429	1184.548072
9829.9	10034.575	10761.25	5793.428571	9104.788393	1121.72705
9907.25	10188.6625	11117.3625	5741.571429	9238.711607	1194.036183
9651.35	10461.8875	11746.4625	5730.571429	9397.567857	1296.191554
9533.1	10773.2	12881.95	5917.285714	9776.383929	1460.308443

9559.65	10658.6125	12960.15	6141.285714	9829.924554	1419.04134
9345.2	10634.1	13321.375	6273.142857	9893.454464	1463.626606
9347.8	10686.95	13474.0625	6481.428571	9997.560268	1453.349479
9185.3	10898.525	13880.8375	6642.285714	10151.73705	1519.707528
9102.6	10864.5125	13712.875	6682.285714	10090.5683	1480.781522
8807.35	10685.6	13717.275	6896.571429	10026.69911	1453.129162
8973.3	10608.2125	13768.8375	6961.714286	10078.01607	1438.604807
9318.2	10629.4625	13520.9625	6966.285714	10108.72768	1366.698782
9648.85	10595.375	13796.3625	7044.428571	10271.25402	1394.37063
9825.45	10582.75	13906.8375	7027	10335.50938	1414.858867
9690.25	10788.2125	14075.7375	7086	10410.05	1447.6329
10195.5	10737.6	14076.075	7050.571429	10514.93661	1438.609035
10381.05	10792.15	14585.525	6733	10622.93125	1605.2221
9774.9	10828.3	14804.05	6296	10425.8125	1751.427945
9649.25	10781.1875	14927.85	6717	10518.82188	1700.94017
9283.65	10874.675	15257.475	7003.571429	10604.84286	1742.471944
9236.5	10871.525	15774.6875	7129.142857	10752.96384	1840.821971
9302.85	10720.525	15967.3125	7116.142857	10776.70759	1882.319628
9437.55	10854.95	16076.75	6953.285714	10830.63393	1925.634898
9620.6	10904.65	16143.0125	6767.857143	10859.02991	1962.013346
9645.95	10847.475	16222.8875	6637.428571	10838.43527	2001.309695
9398.05	10910.7125	16029.2875	6713	10762.7625	1958.340949
9420.4	11009.925	16074.5375	6881.714286	10846.6442	1938.907998
9291.1	11243.55	16422.2125	7052.571429	11002.35848	1999.212643
9952.65	11026.475	15325.6	7360.428571	10916.28839	1658.988345
9767.2	11128.9375	13323.1625	7487.857143	10426.78929	1223.191525
9934.8	11044.7875	13885.9625	7592.285714	10614.45893	1306.502503
9884.45	10877.425	14301.9625	7530	10648.45938	1405.614028
9923.75	10997.5875	14719.75	7138.714286	10694.95045	1568.76189
10017.95	11062.45	14931.1125	6962.857143	10743.59241	1644.625356
9722.2	10929.7875	15070.9	6991	10678.47188	1679.992289
9371.25	11015.6375	15180.5625	6856.571429	10606.00536	1748.26693
9511.35	11044.9625	15168.95	7223.142857	10737.10134	1672.982158
9610.05	10861.475	15523.0875	7355.714286	10837.5817	1722.032962
9860.55	11217.0125	15390.225	7251.714286	10929.87545	1699.252097
9866.45	11613.925	15478.7125	7294	11063.27188	1718.505355
9543.05	11790.7875	15364.2875	7223.142857	10980.31696	1733.449205
9355.95	12108.9875	15528.175	7246.142857	11059.81384	1791.51368
9136.05	12178.1375	15477.45	7236	11006.90938	1804.563223
9101.7	11916.8375	15600.9375	7140.857143	10940.08304	1836.921864
9379.45	11828.0625	15724.55	7336.857143	11067.22991	1803.556178
9774.1	12190.7375	15848.425	7346.142857	11289.85134	1812.974729
9904.2	12174.425	15711.9375	7374.428571	11291.24777	1769.836948
9990.25	12369.4375	15686.0125	7006.571429	11263.06786	1837.668819
9887.6	12603.55	15679.85	6924.142857	11273.78571	1871.331508
9935.75	12910.7875	15666.8	6825	11334.58438	1904.940886
9844	12749.8875	15631.8125	6786	11252.925	1900.746368
10363.4	12651.225	15929.375	7189.142857	11533.28571	1844.261347
10919.25	12471.8625	15907.2875	7501.428571	11699.95714	1744.864188
10927.55	12629.725	16072.2125	7654.142857	11820.90759	1753.277768
11013.15	12640.2625	16090.625	8240.428571	11996.11652	1639.39366
11065.5	12893.6125	16227.9625	8279	12116.51875	1666.809202
11081.2	13104.7125	16180.7875	8123.714286	12122.60357	1695.804422
11177.1	13427.85	16033.2125	8160.714286	12199.7192	1672.405624
11099.5	13362.025	16159.3125	8237.571429	12214.60223	1681.704123

11089.7	13728.5	16045.6875	8440.285714	12326.0433	1643.935688
11255.75	13628.7875	16349.35	8255.857143	12372.43616	1722.098361
11667.2	13627.425	16270.2	8141.857143	12426.67054	1711.504001
11554.15	13604.15	16202.5125	8021.285714	12345.52455	1726.890492
11542.3	13488	12023.8875	8165.857143	11305.01116	1125.196924
11205.9	13356.575	11278.9625	8217.714286	11014.78795	1057.272422
11443.9	13342.7	11307.675	8133.714286	11056.99732	1079.450224
11662.95	13299.8625	11899.4875	8401.714286	11316.00357	1036.404185
11768.3	13105.725	12170.75	8113.285714	11289.51518	1095.173557
12027.6	13272.1625	12509.9625	7944.571429	11438.57411	1192.50876
11823.8	13405.15	12770.1875	7953.571429	11488.17723	1222.170738
11822.9	13718.125	13205.4375	7685.285714	11607.93705	1367.427739
11736.1	13547.2875	13170.75	7608.285714	11515.6058	1359.626199
12002	13674.8375	13115.9625	7355.428571	11537.05714	1436.582645
12418.9	13822.5	13266.3375	7381.142857	11722.22009	1475.51654
12452.75	13840.8375	13142.6125	7214.571429	11662.69286	1509.537754
12368.4	14364.1625	11762.625	6942	11359.29688	1573.814151
12505.55	13992.675	11532.875	7126.714286	11289.45357	1476.875897
12884.45	14145.1375	11546.2	7265.714286	11460.37545	1495.506707
12554.95	13948.45	11510.6625	7189.142857	11300.80134	1458.672612
12517.1	14252.2875	11810.475	7109.142857	11422.25134	1526.472531
12893.75	14126.0875	12319.525	7153.571429	11623.23348	1536.803805
13095.85	14025.2375	12292.3875	7204.428571	11654.47589	1525.011538
13366.6	14131.1625	12273.65	7052.857143	11706.06741	1597.210341
14081.65	13872.95	12053.2375	7052.714286	11765.13795	1635.518212
14249.65	13834.7375	12085.2625	7153.285714	11830.73393	1628.150583
14315.7	13914.775	12009.975	7308.857143	11887.32679	1606.885434
13881.35	13533.1875	12279.075	7603.428571	11824.26027	1448.399321
14440.05	13419.3875	12210.2	7437.285714	11876.7308	1548.393506
14517.5	13491.5375	12150.25	7677.142857	11959.10759	1507.356144

OPN/ Uncoated

FLOW/ uncoated surface			
Res. (ohm)	Res. (ohm)		
Average	Average	Average	Standard Error
1835.428571	2812.5625	2323.995536	488.5669643
1823.571429	2761.525	2292.548214	468.9767857
1820.142857	2751.35	2285.746429	465.6035714
1817	2758.4	2287.7	470.7
1831	2772.2125	2301.60625	470.60625
1831.714286	2797.3625	2314.538393	482.8241071
1828.285714	2825.1875	2326.736607	498.4508929
1814.428571	2803.275	2308.851786	494.4232143
1807.285714	2811.7375	2309.511607	502.2258929
1797.285714	2812.2	2304.742857	507.4571429
1805.428571	2813.2625	2309.345536	503.9169643
1753.285714	2832.8875	2293.086607	539.8008929
1718.428571	2836.175	2277.301786	558.8732143
1713.857143	2815.85	2264.853571	550.9964286
1743.857143	2812.6	2278.228571	534.3714286

1882.142857	2848.3875	2365.265179	483.1223214
1928.428571	2869.5625	2398.995536	470.5669643
2022.714286	2894.5	2458.607143	435.8928571
2031.714286	2890.45	2461.082143	429.3678571
2174.285714	2899.3625	2536.824107	362.5383929
2228.571429	2911.5	2570.035714	341.4642857
2280.285714	2924.2125	2602.249107	321.9633929
2436.571429	2971.8125	2704.191964	267.6205357
2479.857143	2985.4125	2732.634821	252.7776786
2663.714286	2991.4875	2827.600893	163.8866071
2652.571429	2945.65	2799.110714	146.5392857
2679.714286	2950.575	2815.144643	135.4303571
2727.428571	2931.1125	2829.270536	101.8419643
2857	2926.05	2891.525	34.525
3186	2951.8125	3068.90625	117.09375
3076	2987.8625	3031.93125	44.06875
3056.285714	3000.2875	3028.286607	27.99910714
3046.428571	2994.9875	3020.708036	25.72053571
3045.142857	3010.3	3027.721429	17.42142857
3040.714286	3006.6375	3023.675893	17.03839286
3041.571429	3054.6375	3048.104464	6.533035715
3041.428571	3080.5625	3060.995536	19.56696429
3042.142857	3081.8625	3062.002679	19.85982143
3039.571429	3101.2	3070.385714	30.81428571
3038.571429	3107.2	3072.885714	34.31428571
3035	3105.325	3070.1625	35.1625
3043	3114.95	3078.975	35.975
3047.428571	3040.7875	3044.108036	3.320535714
3048.571429	3005.525	3027.048214	21.52321429
3045.142857	2997.85	3021.496429	23.64642857
3041.857143	3039.9125	3040.884821	0.972321429
3044.571429	3030.9875	3037.779464	6.791964286
3049	3058.3375	3053.66875	4.66875
3056	3070.5125	3063.25625	7.25625
3057.571429	3087.65	3072.610714	15.03928571
3057.571429	3096.2875	3076.929464	19.35803571
3061.428571	3075.375	3068.401786	6.973214286
3063.428571	3065.825	3064.626786	1.198214285
3068.428571	3080	3074.214286	5.785714286
3060	3078.875	3069.4375	9.4375
3066.428571	3100.875	3083.651786	17.22321429
3065	3114.925	3089.9625	24.9625
3070.714286	3162.5625	3116.638393	45.92410714
3073.714286	3190.35	3132.032143	58.31785714
3070.571429	3181.8625	3126.216964	55.64553571
3075.428571	3194.025	3134.726786	59.29821429
3082	3221.4	3151.7	69.7
3095.571429	3257.75	3176.660714	81.08928571
3090.142857	3320.4125	3205.277679	115.1348214
3103.285714	3319.075	3211.180357	107.8946429
3115	3330.6625	3222.83125	107.83125
3122.571429	3325.8	3224.185714	101.6142857
3123.714286	3346.25	3234.982143	111.2678571
3128.142857	3354.675	3241.408929	113.2660714
3136.428571	3388.1	3262.264286	125.8357143

3134.571429	3379.1125	3256.841964	122.2705357
3128.142857	3440.225	3284.183929	156.0410714
3120.571429	3487.2375	3303.904464	183.3330357
3127.571429	3527.15	3327.360714	199.7892857
3132.571429	3522.7125	3327.641964	195.0705357
3128	3505.475	3316.7375	188.7375
3132.428571	3502.975	3317.701786	185.2732143
3144.571429	3514.475	3329.523214	184.9517857
3150.142857	3451.275	3300.708929	150.5660714
3165.142857	3540.8375	3352.990179	187.8473214
3176.285714	3552.525	3364.405357	188.1196429
3179.142857	3483.8625	3331.502679	152.3598214
3190.714286	3499.7375	3345.225893	154.5116071
3191.714286	3566.35	3379.032143	187.3178571
3193.428571	3582.6125	3388.020536	194.5919643
3188	3597.2875	3392.64375	204.64375
3180.714286	3615.5375	3398.125893	217.4116071
3177.857143	3647.025	3412.441071	234.5839286
3165.428571	3674.6625	3420.045536	254.6169643
3161.142857	3674.875	3418.008929	256.8660714
3171.857143	3657.9	3414.878571	243.0214286
3175.285714	3669.3	3422.292857	247.0071429
3182.142857	3681.1375	3431.640179	249.4973214
3175	3685.7375	3430.36875	255.36875
3170.857143	3694.7125	3432.784821	261.9276786
3175.142857	3682.9375	3429.040179	253.8973214
3173	3657.475	3415.2375	242.2375
3174.714286	3664.425	3419.569643	244.8553571
3171.428571	3656.075	3413.751786	242.3232143
3185.571429	3654.1	3419.835714	234.2642857
3190.428571	3691.775	3441.101786	250.6732143
3193.571429	3709.2625	3451.416964	257.8455357
3176.857143	3779.0625	3477.959821	301.1026786
3156.428571	3797.075	3476.751786	320.3232143
3135.571429	3843.9125	3489.741964	354.1705357
3133	3863.9	3498.45	365.45
3115.857143	3936.475	3526.166071	410.3089286
3120.571429	3973.9125	3547.241964	426.6705357
3129.714286	3960.05	3544.882143	415.1678571
3133.428571	3993.35	3563.389286	429.9607143
3133.285714	4031.3125	3582.299107	449.0133929
3148.714286	4063.7625	3606.238393	457.5241071
3152.714286	4243.6125	3698.163393	545.4491071
3143.285714	4261.9125	3702.599107	559.3133929
3147.142857	4316.6625	3731.902679	584.7598214
3138.571429	4380.3875	3759.479464	620.9080357
3131.428571	4414.15	3772.789286	641.3607143
3135.285714	4473.6	3804.442857	669.1571429
3138.142857	4592.1125	3865.127679	726.9848214
3150	4575.5375	3862.76875	712.76875
3159.571429	4558.775	3859.173214	699.6017857
3164.428571	4548.7	3856.564286	692.1357143
3156.571429	4642.125	3899.348214	742.7767857
3166.285714	4705.6875	3935.986607	769.7008929
3182.285714	4737.35	3959.817857	777.5321429

3183.857143	4800.3375	3992.097321	808.2401786
3184.142857	4840.075	4012.108929	827.9660714
3200.857143	4911.9	4056.378571	855.5214286
3210.142857	5007.9875	4109.065179	898.9223214
3222.714286	5043.525	4133.119643	910.4053571
3223.285714	4971.725	4097.505357	874.2196429
3229.857143	4892.7625	4061.309821	831.4526786
3222.285714	5068.275	4145.280357	922.9946429
3233.285714	5068.5	4150.892857	917.6071429
3253.571429	5129.1	4191.335714	937.7642857
3262.571429	4988.5	4125.535714	862.9642857
3274.714286	4910.95	4092.832143	818.1178571
3276.571429	4911.125	4093.848214	817.2767857
3305	4876.1625	4090.58125	785.58125
3324.285714	4989.525	4156.905357	832.6196429
3330.714286	5073.3375	4202.025893	871.3116071
3307.428571	5131.675	4219.551786	912.1232143
3303	5091	4197	894
3282.571429	5065.9875	4174.279464	891.7080357
3300	5116.125	4208.0625	908.0625
3332	5108.4875	4220.24375	888.24375
3359	5211.9375	4285.46875	926.46875
3381.142857	5270.2875	4325.715179	944.5723214
3423.571429	5244.5	4334.035714	910.4642857
3427.714286	5073.975	4250.844643	823.1303571
3410.571429	5192.05	4301.310714	890.7392857
3404.714286	5241.1	4322.907143	918.1928571
3405	5304.3875	4354.69375	949.69375
3385.714286	5390.7	4388.207143	1002.492857
3398.428571	5394.0375	4396.233036	997.8044643
3408.285714	5454.1125	4431.199107	1022.913393
3402.857143	5550.825	4476.841071	1073.983929
3404.714286	5527.225	4465.969643	1061.255357
3414.142857	5516.0875	4465.115179	1050.972321
3423.857143	5472.35	4448.103571	1024.246429
3431.857143	5505.6	4468.728571	1036.871429
3432.857143	5581.6	4507.228571	1074.371429
3438.571429	5643.725	4541.148214	1102.576786
3453.142857	5593.5625	4523.352679	1070.209821
3475.285714	5561.55	4518.417857	1043.132143
3488.857143	5588.1625	4538.509821	1049.652679
3497.571429	5608.525	4553.048214	1055.476786
3499.285714	5692.5375	4595.911607	1096.625893
3549.285714	5700.225	4624.755357	1075.469643
3555.857143	5761.5125	4658.684821	1102.827679
3559.142857	5791.325	4675.233929	1116.091071
3571.428571	5862.875	4717.151786	1145.723214
3565.857143	5941.1625	4753.509821	1187.652679
3565.714286	5923.025	4744.369643	1178.655357
3578.857143	5884.4	4731.628571	1152.771429
3585.142857	5966.9125	4776.027679	1190.884821
3598.857143	6014.8125	4806.834821	1207.977679
3619.714286	6023.125	4821.419643	1201.705357
3627.142857	6163.3125	4895.227679	1268.084821
3631.714286	6098.3625	4865.038393	1233.324107

3610	6097.8375	4853.91875	1243.91875
3608.714286	6026.4125	4817.563393	1208.849107
3616	6022.3875	4819.19375	1203.19375
3631.142857	6068.5	4849.821429	1218.678571
3657.571429	6071.5	4864.535714	1206.964286
3682.285714	6102.1125	4892.199107	1209.913393
3672.142857	6195.0125	4933.577679	1261.434821
3694.142857	6300.4625	4997.302679	1303.159821
3728.285714	6280.9375	5004.611607	1276.325893
3757.142857	6267.6625	5012.402679	1255.259821
3767.428571	6438.6	5103.014286	1335.585714
3776.428571	6636.1875	5206.308036	1429.879464
3778.857143	6619.775	5199.316071	1420.458929
3753.857143	6591.5625	5172.709821	1418.852679
3780.714286	6601.675	5191.194643	1410.480357
3796.857143	6641.0375	5218.947321	1422.090179
3796.857143	6553.25	5175.053571	1378.196429
3801	6629.4625	5215.23125	1414.23125
3799	6611.2125	5205.10625	1406.10625
3817.571429	6611.8375	5214.704464	1397.133036
3780.571429	6688.9125	5234.741964	1454.170536
3798.714286	6715.6625	5257.188393	1458.474107
3822.714286	6914.05	5368.382143	1545.667857
3838.285714	6868	5353.142857	1514.857143
3856	6900.9125	5378.45625	1522.45625
3857	7047.9375	5452.46875	1595.46875
3860.714286	7104.3625	5482.538393	1621.824107
3888.285714	7060.9625	5474.624107	1586.338393
3909.428571	6947.1625	5428.295536	1518.866964
3928.285714	6939.0125	5433.649107	1505.363393
3943.857143	7095.45	5519.653571	1575.796429
3955	7087.875	5521.4375	1566.4375
3963.428571	7023.3	5493.364286	1529.935714
3974.857143	7036.8375	5505.847321	1530.990179
4007.857143	7154.875	5581.366071	1573.508929
4056.142857	7138.525	5597.333929	1541.191071
4086.857143	7418.3	5752.578571	1665.721429
4095.142857	7328.4	5711.771429	1616.628571
4094.285714	7208.8	5651.542857	1557.257143
4091.428571	7023.2125	5557.320536	1465.891964
4104	6948.9	5526.45	1422.45
4103	7089.4	5596.2	1493.2
4101.571429	7082.3625	5591.966964	1490.395536
4099.714286	7115.1125	5607.413393	1507.699107
4074.428571	7192.975	5633.701786	1559.273214
4095.428571	7121.7875	5608.608036	1513.179464
4082.285714	7354.7875	5718.536607	1636.250893
4067.714286	7362.6	5715.157143	1647.442857
4058.571429	7510.45	5784.510714	1725.939286
4048.142857	7697.4125	5872.777679	1824.634821
4068.285714	7801.8375	5935.061607	1866.775893
4074	7723.8625	5898.93125	1824.93125
4108.714286	7725.8125	5917.263393	1808.549107
4124.714286	7757.4625	5941.088393	1816.374107
4107.714286	7788.0375	5947.875893	1840.161607

4099.285714	7856.075	5977.680357	1878.394643
4094.857143	7995.8625	6045.359821	1950.502679
4111.285714	8005.4375	6058.361607	1947.075893
4129.142857	8085.5875	6107.365179	1978.222321
4137.142857	8250.4	6193.771429	2056.628571
4144.142857	8286.85	6215.496429	2071.353571
4163.428571	8158.45	6160.939286	1997.510714
4186.571429	8161.9125	6174.241964	1987.670536
4171.857143	8170.5125	6171.184821	1999.327679
4134.571429	8294.0875	6214.329464	2079.758036

OPN/ Static

	STATIC/OPN			
Res. (ohm)	Res. (ohm)	Res. (ohm)		
Average	Average	Average	Average	Standard Error
2361.025	2400.257143	2318.7	2359.994048	23.54916159
2195.9	2391.628571	2318.9125	2302.147024	57.12042633
2177.95	2387.785714	2308.8	2291.511905	61.18800379
2156.8125	2390.914286	2308.125	2285.283929	68.53757467
2146.8625	2390.942857	2306.35	2281.385119	71.55706149
2132.125	2423.4	2313.9375	2289.820833	84.94408281
2121.75	2437.714286	2329.775	2296.413095	92.72381927
2103.175	2463.642857	2330.0375	2298.951786	105.2124996
2097.975	2479.4	2321.8	2299.725	110.6597441
2084.4875	2497.171429	2325.5625	2302.407143	119.6928488
2077.75	2520.4	2316.6	2304.916667	127.9155071
2076.5	2548.614286	2321.9375	2315.683929	136.3235185
2074.0875	2583.671429	2324.125	2327.294643	147.1127459
2070.775	2623	2333.4375	2342.404167	159.4766582
2069.6875	2651.557143	2325.9375	2349.060714	168.3687249
2071.95	2676.657143	2303.7625	2350.789881	176.1404393
2073.5875	2721.514286	2287.9375	2361.013095	190.5757171
2075.7125	2758.314286	2292.3	2375.442262	201.3875006
2082.8375	2796.185714	2302.1	2393.707738	210.9584493
2086.975	2842.8	2308.5	2412.758333	224.3287823
2088.725	2891.342857	2314.3	2431.455952	238.9860484
2094.35	2936.257143	2326.25	2452.285714	251.0747965
2092.5875	2984.014286	2336.45	2471.017262	265.9835142
2094.6	3046.457143	2331.4625	2490.839881	286.0995557
2096.2125	3120.457143	2339.6875	2518.785714	308.9371025
2099.75	3185.242857	2341.6625	2542.218452	329.0089681
2102.7375	3301.9	2347.6	2584.079167	365.8048079
2107.6125	3367.628571	2352.3	2609.180357	385.7463603
2115.3	3440.814286	2346.025	2634.046429	408.8456465
2116.675	3518.914286	2351.525	2662.371429	433.6042282
2127.35	3582.471429	2347.65	2685.82381	452.8118583
2137.5625	3663.157143	2352.25	2717.656548	476.7952783
2149.5	3747.585714	2359.55	2752.211905	501.3671363
2150.475	3822.285714	2374.5625	2782.441071	523.9311223
2152.7125	3897.814286	2377.9375	2809.488095	548.0334533
2160.7625	3977.771429	2377.325	2838.619643	572.996487

2165.8125	4070.471429	2378.4125	2871.565476	602.5864535
2171.7	4167.085714	2379.8625	2906.216071	633.2922177
2172.3375	4269.557143	2375.0625	2938.985714	667.8546751
2166.55	4351.028571	2377.225	2964.934524	695.7103134
2171.3	4552.885714	2366.7375	3030.307738	763.3766489
2174.5875	4671.271429	2372.95	3072.93631	801.2164262
2182.4375	4764.3	2381.7125	3109.483333	829.4056671
2189.7875	4883.257143	2388.15	3153.731548	866.6566042
2198.9625	4978.942857	2404.325	3194.076786	894.3999122
2211.6375	5047.085714	2409.425	3222.716071	913.9699884
2214.5125	5115.171429	2401.2125	3243.632143	937.3204176
2212.7625	5187.957143	2410.1625	3270.294048	960.5233817
2215.8875	5281.514286	2412.4375	3303.279762	990.7432982
2217.35	5333.042857	2416.6375	3322.343452	1006.994364
2215.275	5449.114286	2422.2625	3362.217262	1045.157938
2211.3625	5519.885714	2430.1125	3387.120238	1068.250801
2214.45	5609.242857	2440.875	3421.522619	1095.81126
2212.85	5686.071429	2451.975	3450.29881	1120.015565
2204.9	5725.257143	2449.8625	3460.006548	1134.830656
2202.425	5809.485714	2442.55	3484.820238	1164.397868
2205.3875	5866.785714	2438.05	3503.407738	1183.596152
2213.4375	5963.514286	2429.6375	3535.529762	1215.595498
2209.4	6057.828571	2436.6625	3567.96369	1246.659858
2210.375	6077.257143	2434.8	3574.144048	1253.232224
2219.55	6099.5	2429.6375	3582.895833	1259.762754
2227.8875	6199.414286	2434.4375	3620.579762	1290.795149
2246.8875	6280.757143	2447.225	3658.289881	1312.508372
2248.5125	6319.985714	2437.75	3668.749405	1326.743279
2250.2875	6346.885714	2437.1125	3678.095238	1335.484662
2242.25	6435.485714	2442.8125	3706.849405	1365.546095
2246.85	6486.314286		4366.582143	1730.754047
2245.6625	6546.685714	2421.925	3738.091071	1405.218846
2246.875	6633.014286	2430.225	3770.038095	1432.466266
2254.325	6672.242857	2439.2	3788.589286	1442.814164
2265.75	6714.8	2430.9125	3803.820833	1456.270287
2274.05	6838.242857	2406.5	3839.597619	1499.810066
2271.6125	7100.828571	2422.025	3931.48869	1585.264693
2267.6125	7126.814286		4697.213393	1983.760822
2256.3875	7201.642857	2424.1	3960.710119	1621.189443
2253.0125	7209.7	2415.325	3959.345833	1625.852391
2246.325	7299.028571	2413.2625	3986.205357	1657.112475
2247.775	7345.071429	2403.25	3998.69881	1673.788158
2245.675	7410.328571	2417.4625	4024.48869	1693.646117
2246.025	7512.728571	2422.6875	4060.480357	1726.877308
2247.65	7548.371429	2425.8125	4073.944643	1737.974548
2239.3125	7571.114286	2419.525	4076.650595	1748.00615
2239.675	7485.857143	2418.5625	4048.031548	1719.688325
2229.0875	7505.942857	2438.175	4057.735119	1725.160075
2229.7875	7582.971429	2438.9875	4083.915476	1750.569962
2231.4	7724.114286	2433.275	4129.596429	1798.203488
2231.1125	7707.457143	2444.775	4127.781548	1790.900234
2233.525	7667.571429	2428.45	4109.84881	1779.75107
2230.25	7573.314286	2431.6125	4078.392262	1748.427549
2239.3125	7605.671429	2420.0625	4088.34881	1759.435179

2242.45	7592.471429	2419.5375	4084.819643	1754.570772
2244.1	7502.685714	2408.875	4051.886905	1726.054945
2251.8875	7471.628571	2405.7875	4043.10119	1714.839283
2251.9875	7514.514286	2410.3375	4058.946429	1728.388517
2252.6625	7512.785714	2421.9	4062.449405	1725.859768
2258.1125	7513.957143	2440.15	4070.739881	1722.410447
2256.475	7495.642857	2448.2875	4066.801786	1715.314483
2257.4	7443.414286	2457.6375	4052.817262	1696.283673
2266.65	7446.585714	2458.4	4057.211905	1695.590667
2274.625	7488.914286	2461	4074.846429	1707.881574
2274.0875	7537.557143	2465.4625	4092.369048	1723.479703
2278	7473.342857	2472.375	4074.572619	1700.311222
2295.0875	7407.657143	2476.05	4059.598214	1674.844351
2305.325	7425.085714	2454.5625	4061.657738	1682.265711
2305.5	7511.314286	2431.3125	4082.708929	1714.687359
2310.95	7533.3	2420.025	4088.091667	1722.891918
2298.725	7597.028571	2387.925	4094.559524	1751.423824
2285.5375	7690.985714	2363.075	4113.199405	1789.033181
2267.9	7712	2343.175	4107.691667	1802.28517
2262.4	7757.3	2339.675	4119.791667	1818.890964
2247.3	7768.642857	2328.2	4114.714286	1827.113544
2241.3375	7880.685714	2325.425	4149.149405	1865.926052
2242.0875	7839.471429	2327.45	4136.33631	1851.731529
2244.7125	7861.985714	2333.5875	4146.761905	1857.789067
2242.3875	7855.114286	2328.9125	4142.138095	1856.656115
2239.075	7837.571429	2332.9875	4136.544643	1850.711966
2232.4125	7763.428571	2328.1375	4107.992857	1827.926741
2229.5	7738.1	2319.6375	4095.745833	1821.36296
2213.6125	7753.057143		4983.334821	2261.468806
2190.5375	7737.514286	2312.0125	4080.021429	1829.082606
2191.225	7814.7	2300.775	4102.233333	1856.502703
2187.35	7849.642857	2303.2625	4113.418452	1868.41185
2177.05	7840.842857	2308.35	4108.747619	1866.432522
2171.8625	7824.614286	2305.4375	4100.638095	1862.387318
2171.825	7921.9	2317.8625	4137.195833	1892.821612
2175.95	7952.857143	2333.425	4154.077381	1899.933802
2176.6	7986.814286	2352.375	4171.929762	1908.117061
2173.8875	7844.085714	2350.3125	4122.761905	1861.358788
2172.95	8025.428571	2346.5875	4181.655357	1922.54015
2172.7125	7971.9	2349.15	4164.5875	1904.337497
2174.5375	7980.342857	2339.275	4164.718452	1908.404815
2169.825	7955.157143	2354.9375	4159.973214	1898.34423
2166.475	7851.328571	2351.2125	4123.005357	1864.924259
2163.125	7845.371429	2350.0375	4119.51131	1863.711288
2155.2125	7672.714286	2354.625	4060.850595	1806.849083
2154.175	7529.314286	2339.9875	4007.825595	1761.561194
2146.3625	7412.014286	2344.275	3967.550595	1723.179225
2137.725	7414.042857	2340.1125	3963.960119	1726.030451
2144.7375	7350.971429	2353.9625	3949.890476	1701.612716
2152.5875	7356.514286	2363.25	3957.450595	1700.61951
2149.5	7407.428571	2368.55	3975.159524	1717.299123
2147.3875	7474.042857	2371.0875	3997.505952	1739.467549
2160.675	7369.3	2348.4375	3959.470833	1705.775962
2162.7875	7382.671429	2339.875	3961.777976	1711.210488

2157.675	7352.742857	2328.025	3946.147619	1704.007347
2161.525	7339.871429	2314.175	3938.52381	1701.244615
2168.075	7352.828571	2321.8625	3947.58869	1703.198622
2170.7	7275.485714	2340.625	3928.936905	1673.993262
2173.0125	7393.785714	2353.9125	3973.570238	1710.90489
2184.3125	7416.542857	2357.7	3986.185119	1715.909037
2182.575	7319.757143	2357.9	3953.410714	1683.933978
2180.2125	7405.042857	2359.5375	3981.597619	1712.505215
2184.2375	7434.042857	2358.5875	3992.289286	1721.612637
2189.025	7418.628571	2359.725	3989.12619	1715.459079
2188.775	7420.628571	2360.2375	3989.880357	1716.088074
2187.775	7478.142857	2353.425	4006.447619	1736.506152
2193.1625	7366.571429	2357.625	3972.452976	1697.723184
2207.7125	7261.8	2355.5	3941.670833	1660.612693
2208.8375	7133	2338.075	3893.304167	1620.277487
2208.1625	7043.742857	2331.35	3861.085119	1591.726159
2212.3	7028.428571	2354.3125	3865.01369	1582.238622
2208.475	7071.771429	2362.275	3880.840476	1596.083108
2212.6875	7050.828571	2383.3	3882.272024	1585.043648
2212.25	7036.528571	2387.75	3878.842857	1579.655486
2218.175	7035.014286	2409.6875	3887.625595	1574.665143
2227.675	6931.485714	2417.8625	3859.007738	1537.219731
2227.5125	6936.628571	2421.5875	3861.909524	1538.380013
2239.0625	6965.471429	2422.4875	3875.67381	1545.805958
2249.8875	6986.414286	2423.0625	3886.454762	1550.785734
2251.3375	6990.185714	2439.45	3893.657738	1549.216007
2248.5625	6921.285714	2448.1625	3872.670238	1525.396373
2256.7	6795.5	2454.4625	3835.554167	1481.073598
2254.7625	6696.128571	2444.85	3798.580357	1449.812925
2260.975	6592.542857	2446.4875	3766.668452	1413.951712
2266.2625	6481.614286	2450.4625	3732.779762	1375.445484
2276.425	6525.442857	2441.5125	3747.793452	1389.642116
2278.225	6433.214286	2460.9625	3724.133929	1355.566983
2278.9	6279.814286	2466.3375	3675.017262	1303.522005
2277.3875	6261.357143	2477.9625	3672.235714	1295.854919
2270.2375	6196.814286	2494.6875	3653.913095	1273.100454
2271.975	6185.328571	2515.5875	3657.630357	1265.804153
2286.6375	6185.257143	2524.175	3665.356548	1261.814867
2290.9125	6263.1	2490.575	3681.529167	1292.071625
2289.3125	6272.657143	2475.2	3679.056548	1297.910061
2288.1375	6194.542857	2469.1625	3650.614286	1273.037306
2299.275	6314.157143	2462.9625	3692.131548	1311.864077
2294.275	6211.585714	2455.5875	3653.816071	1279.732341
2288.975	6232.185714	2462.6375	3661.266071	1286.437008
2290.4875	6204.857143	2467.2375	3654.194048	1276.351808
2285.4375	6190.7	2466.5	3647.545833	1272.650874
2288.25	6110.271429	2469.575	3622.69881	1244.887256
2290.9625	6072.9	2471.1	3611.654167	1231.721109
2294.95	6074.342857	2487.075	3618.789286	1229.028819
2291.7	6056.9		4174.3	1537.136463
2311.675	6044.6	2479.625	3611.966667	1217.282561
2324.425	6008.771429	2489.2625	3607.48631	1201.585136
2326.55	6017	2489.55	3611.033333	1203.903229
2336.6625	5986.685714	2495.8125	3606.386905	1191.035823

2339.4125	6052.442857	2500.5125	3630.789286	1211.719552
2343.3625	6061.557143	2508.825	3637.914881	1212.762112
2369.8	5934.042857	2495.475	3599.772619	1167.698835
2383.575	5844.671429	2499.525	3575.92381	1134.867528
2388.8125	5831	2497.2625	3572.358333	1129.754691
2391.0125	5807.8	2506.95	3568.5875	1120.10637
2388	5820.942857	2527.65	3578.864286	1121.763904
2380	5811.385714	2530.8625	3574.082738	1119.498895
2382.7875	5913.042857	2499.1	3598.310119	1157.853313
2394.6	5844.514286	2475.725	3571.613095	1136.691864
2394.0875	5919.342857	2475.575	3596.335119	1161.742049
2399.5	5877.357143	2483.1625	3586.673214	1145.596569
2412.825	5846.714286	2482.425	3580.654762	1133.20789
2417.6625	5822.357143	2491.45	3577.156548	1122.802362
2424.5375	5783.342857	2513.65	3573.843452	1105.049165
2432.225	5715.357143	2535.15	3560.910714	1077.632892
2441.0625	5590.271429	2548.2625	3526.532143	1032.333577
2443.2125	5544.914286	2550.9	3513.008929	1016.428172
2446.2375	5478.357143	2550.6125	3491.735714	993.7675886
2441.2625	5434.414286	2520.0875	3465.254762	984.8426723
2440.9375	5346.657143	2512.8875	3433.494048	956.8070116
2444.35	5359	2509.65	3437.666667	960.8515938
2434.6375	5371.871429	2491.5875	3432.69881	969.7256761
2446.825	5445.957143	2509.7125	3467.498214	989.3960293
2450.725	5350.9	2525.675	3442.433333	954.4785905
2458.6125	5299.428571	2531.8625	3429.967857	934.9695026
2453.875	5306.871429	2537.5875	3432.777976	937.3582821
2452.25	5227.385714	2557.625	3412.420238	907.9924252
2461.375	5123.6	2543.8875	3376.2875	873.9808937
2469.5	5068.2	2533.875	3357.191667	855.70598
2470.9	5022.928571	2546	3346.609524	838.4398536
2466.175	4983.342857	2542.0125	3330.510119	826.7062914
2459.7	5000.971429	2536.6375	3332.43631	834.5631447
2444.175	4964.514286	2549.0875	3319.258929	823.1849834
2445.1	4945.414286	2542.725	3311.079762	817.6530768
2439.8	4920.185714	2553.8625	3304.616071	808.4556299
2440.15	4942.757143	2547.5	3310.135714	816.8987192
2449.75	4919.614286	2538.2125	3302.525595	808.9475216
2456.4625	4888.685714	2533.1125	3292.753571	798.2727936
2461.2125	4892.585714	2519.95	3291.249405	800.8476771
2465.375	4843.557143	2515.8	3274.910714	784.4582809
2446.4	4826.842857	2508.4125	3260.551786	783.3501086
2459.1	4805.471429	2507.475	3257.34881	774.1872659
2477.1375	4824.6	2506.6375	3269.458333	777.6174649
2471.2625	4916.485714	2505.75	3297.832738	809.3877192
2480.375	4922.571429	2540.275	3314.407143	804.2680482
2483.525	4910.585714	2549.1125	3314.407738	798.3135409

EPCs migration in response to OPN form

OPN form	Haptotoctic	Chemotactic	Negative
EXP(1)	172	52	40
EXP(2)	137	47	18
EXP(3)	100	60	
Average	136.3333333	53	29
Standard error	20.78728244	3.785938897	11

Crystal violate stained adherent cells

Coating concentration µM	**0**	**1**	**10**	**100**
	Number of cells adhering per field			
EXP(1)	33.25	77	91.875	100.125
EXP(2)	45.875	72.625	86.25	116
EXP(3)	38.875	71.25	87.125	119.75
Average	39.33333333	73.625	88.41666667	111.9583333
Standard error	3.651721436	1.733553672	1.747518081	6.014883161

Adhesion of L-EPCs to OPN serial concentration (absorbance readings of Crystal violate stain)

0	0.000001	0.00001	0.0001	0.001	0.01	0.1	1	10
	0.157	0.162	0.207	0.191	0.212	0.227	0.245	0.274
	0.187	0.194	0.192	0.213	0.203	0.224	0.231	0.236
0.197	0.172	0.178	0.1995	0.202	0.2075	0.2255	0.238	0.255
	0.021213203	0.022627417	0.010606602	0.015556349	0.006363961	0.0021213	0.009899495	0.026870058

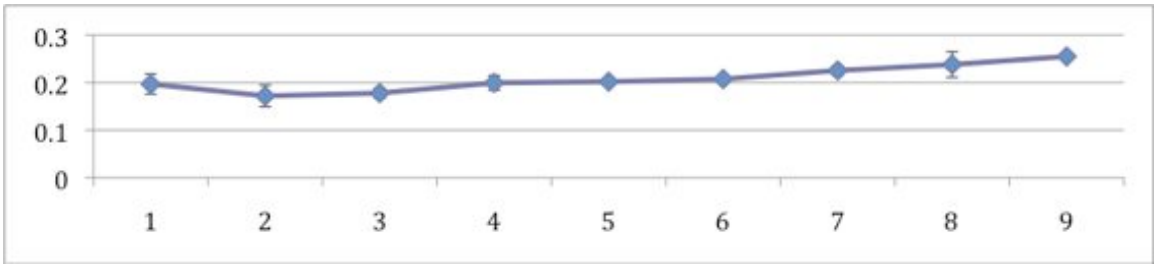

Crystal violate spreading assay

Coating concentration µM	0	1	10	100
	Percentage of spreading cells *vs* total number of adhering cells			
EXP(1)	30.16483	58.89303	61.1194	79.62067
EXP(2)	46.01434	60.18884	69.0309	86.79401
EXP(3)	38.25508	57.05471	69.11044	74.31461
Average	38.14475	58.7121933	66.42024667	80.24309667
Standard error	4.575691	0.90925222	2.650522791	3.615910089

Adhesion and ECS

		Osteopontin	Uncoated	Fibronectin
	0	244.3333	231.5	259
Averages	5.1	649.3333	392	966
	10.1	1011.5	476	1192
	15	1166.667	460.5	1455
	20	1265.333	469.5	1507
Standard Errors	0	8.758065	11.5	27
	5.1	30.03578	97	359
	10.1	159.1496	144	443
	15	196.8549	159.5	496
	20	192.4854	198.5	449

Adhesion Assay
(Crystal violate and Immunocyto chemistry)

Materials:

1- Overnight starved late-EPCs (wash confluent cell culture with PBS then add EBM2 media with 0.5% serum)
2- Recombinant OPN ***(1433OP/ CF, R&D)***
3- Phosphate buffer saline.
4- Circular cover slips size (12)
5- 24 well plate.
6- Countess (invitrogen)
7- 0.5% Crystal violate (0.05 g crystal violate, 2.5 ml of 100% methanol, and 7.8 ml H2O
8- Non serum supplemented EBM-2 media
9- Serum and growth factors supplemented media.

Method:

Wells and cover slips coatings:

1- Thaw the stock OPN solution in ice fro 20 minutes.
2- Prepare OPN solutions
3- Add 300µl of the prepared OPN solution into each well.
4- Incubate overnight at 4 ºC.

Cell culture:

1- Start with preparing dishes first: take the overnight OPN incubated out of 4 ºC.
2- Wash three times with cold dPBS by gently pouring 100µl dPBS on the wells edges. *Note: leave the last wash until usage, and keep the plate covered all the time to avoid evaporation.*
3- **Prepare cell suspension using 1ml only of** TrypLE™ **on the overnight starved L-EPCs.**
4- **Monitor cells detachment under microscope, then as cells look shrinking strike the flask to make single cell suspension.**
5- **Add 2ml of serum supplemented media and quickly centrifuge the suspension at 220 g for 5 min.**
6- **Remove the supernatant and re-suspend the cells in 5 ml dPBS, then re-centrifuge again at 220 g for 5 min.**
7- **Remove the supernatant and suspend the cells in 1ml EBM-2.**
8- Count cell concentration using countess (invitrgen); viable cell count should be at least 3×10^5
9- Incubate the cells for 4 hours.
10- Wash three times with pre-warmed dPBS.
11- Fix in 4% PFA for ten minutes at room temperature.
12- Wash three times in dPBS
13- Stain :
    - Crystal violate:

- Remove the PBS and stained with 200 µl/ well crystal violet 0.05% for 30 min.
- Wash once with PBS, then let it dry overnight. Note: do not uncover the plate completely, instead put the plate inside a folded filter paper.
- After that, remove the CV and add 1% SDS, and agitate. Then read at 570nm (OPTIONAL).

- Immunofluorescence for F-actin :
  - Place each coverslip in a glass Petri-dish and extract it with a solution of 0.1% Triton X-100 in PBS for 3 to 5 minu tes.
  - Wash two or more times with PBS.
  - Incubate fixed cells with PBS containing 1% BSA for 20–30 minutes prior to adding the phallotoxin staining solution.
  - Dilute 5µl methanolic stock solution into 200µl PBS for each coverslip to be stained.
  - Place the staining solution on the coverslip for 20 minutes at room temperature. To avoid evaporation, keep the coverslips inside a covered container during the incubation.
  - Wash two or more times with PBS.
  - Prepare 1:4000 DAPI staining solution.
  - Stain the cells for 5 minutes at room temperature.
  - Wash two or more times with PBS.
  - Remove the coverslips carefully from Petri-dishes and place them on 20µl of 'M' on a glass slide.
  - Let the mounting stand for 5-10 minutes, and then drop nail polish at the edges.
  - After the nail polished dry, cover the rest of the coverslip edges with nail polish.
  - Let it stand for ten minutes, then take pictures using the fluorescent microscope.
- Image J:

Press open on file, and then choose the wanted picture

- Fluorescent Microscope

Haptotactic migration assays

In 24-well Transwell plates

Materials:

- Overnight starved late-EPCs (wash confluent cell culture with PBS then add EBM2 media with 2% serum)
- Recombinant OPN ***(1433OP/ CF, R&D)*** **FN (Roche) , and Collagen type I**
- Phosphate buffer saline.
- 24 well migration plate.
- Countess (invitrogen)
- 0.5% Crystal violates (0.05 g crystals violate, 2.5 ml of 100% methanol, and 7.8 ml H2O.
- DAPI
- Non serum supplemented EBM-2 media
- Serum and growth factors supplemented media.

Method:

Optimization!

Assessment of OPN coating efficiency:

This assay will be applied to determine the followings:

- Filters can be coated or not.
- Wither or not coating the filters with increased protein concentration will result in increase adsorption. Or saturation point will be achieved.

Protein	OPN/ FN/ Col I (1µg/ µl) solutions			
µg/ml	0.1	1	10	100
µg/50µl	0.005	0.05	0.5	5
×2(100µl)	0.010	0.1	1	10

The above diagram will be according to …. How identified FN and Collagen I to be (MSCs) hapotactic agents.

Trans-well coating:

Proteins solutions preparations:

OPN:

OPN in reconstituted at 1µg/ µl concentration. To coat transwells with the above indicated concentrations apply the followings:

- Thaw the stock OPN solution in ice fro 20 minutes.
- To prepare OPN solutions see the above table
- Add 50µl of the prepared OPN solution into each well.
- Incubate overnight at 4 ºC.
- Next day, wash the coated inserts three times with cold dPBS by gently pouring 100µl dPBS on the wells edges.

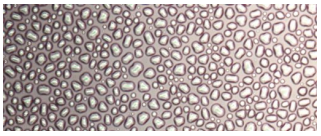

Coated and Uncoated boyden chamber membranes

FN:

FN is reconstituted at 1µg/ µl concentration. To coat transwells with the above indicated concentrations apply the followings:

- Thaw the stock FN solution in ice fro 20 minutes.
- To prepare FN solutions see the above table
- Add 50µl of the prepared FN solution into each well.
- Incubate 45 minutes at 37 ºC.
- Then, wash the coated inserts three times with warm dPBS by gently pouring 100µl dPBS on the wells edges.

Collagen I:

Col I is reconstituted at 10µg/ µl concentration. To coat transwells with the above indicated concentrations apply the followings:

- Thaw the stock Col I solution in ice for ? minutes.
- Prepare a working solution of 1µg/ µl
- To prepare Col I solutions see the above table
- Add 50µl of the prepared Col I solution into each well.
- Incubate overnight at 4 ºC.
- Then, wash the coated inserts three times with warm dPBS by gently pouring 100µl dPBS on the wells edges.

Protein quantification method:

According to … the BCA but not Lowry assay will be used due to the higher sensitivity (1-25 µg/ ml) and compatibility to post-translation glycosylated proteins

Standard Curve:

- The same protein standard curve will be applied for each protein. 0.1, 1, 10, and 100 µg/ ml of OPN, FN and Collagen I.
- The amount of adsorbed proteins will be determine by placing the coated filters in BCA solution in 0.5 ml eppendorf tube and vortex for 5 min to extract all the proteins adsorbed then incubate at 37ºC
- After 15 min, measure the proteins concentrations at 562nm.
- The amount of proteins coating concentration will be determined accordingly.

Cell culture:

- Start with preparing coated inserts first (OPN/ FN / Collagen I over night at 4ºC)
- Wash the coated inserts three times with dPBS by gently pouring 100µl dPBS on the wells edges. *Note: leave the last wash until usage, and keep the plate covered all the time to avoid evaporation and contamination.*
- Block both sides of the membrane were blocked with 1 % BSA in PBS for 1 h at 37 °C.

- **Prepare cell suspension using 1ml only of** TrypLE™ **on the overnight starved L-EPCs.**
- **Monitor cells detachment under microscope, then as cells look shrinking strike the flask to make single cell suspension.**
- **Add 2ml of serum supplemented media and quickly centrifuge the suspension at 220 g for 5 min.**
- **Remove the supernatant and re-suspend the cells in 5 ml dPBS, then re-centrifuge again at 220 g for 5 min.**
- **Remove the supernatant and suspend the cells in 1ml 2% serum EBM-2.**
- Count cell concentration using countess (invitrogen); viable cell count should be at least 3×10^5 / ml.
- At least 3×10^5 / ml cells in 250 µl of serum-free culture medium were added to the upper chambers
- Add 750 µL of the same medium to the bottom chamber and incubate at 37 °C for desired time points see below.
- Remove non migrating cell with PBS wet cotton swabs.
- Fix cells on the other side with 4% PFA for 10 minutes
- Wash with 100 µl PBS three times gently.
- Then, Stain with DAPI 1:4000 for 5 minutes.
- Wash with PBS three times or more gently.
- Cut the filter edges gently in circular motion and directly apply Mowiol medium on microscope slid and coverslip. Let it stand for 5 minutes then gently add nail polish around the slide edges.
- Quantify by performing cell counts on the underside of the filter on whole area at 40× magnification.

Concentration and time points charts will be produced:

Here protein concentration and cells incubation time effects on the migration will be examined.

- Concentration of 0.1, 1, 10, and 100

Proteins	OPN/ FN/ Col I				Negative Ctrls
					BSA
µg/ml	0.1	1	10	100	1%

Cells Pictures

Flow *vs* Static condition (cells were plated in 10μM OPN coated gold electrodes) for 12 hours

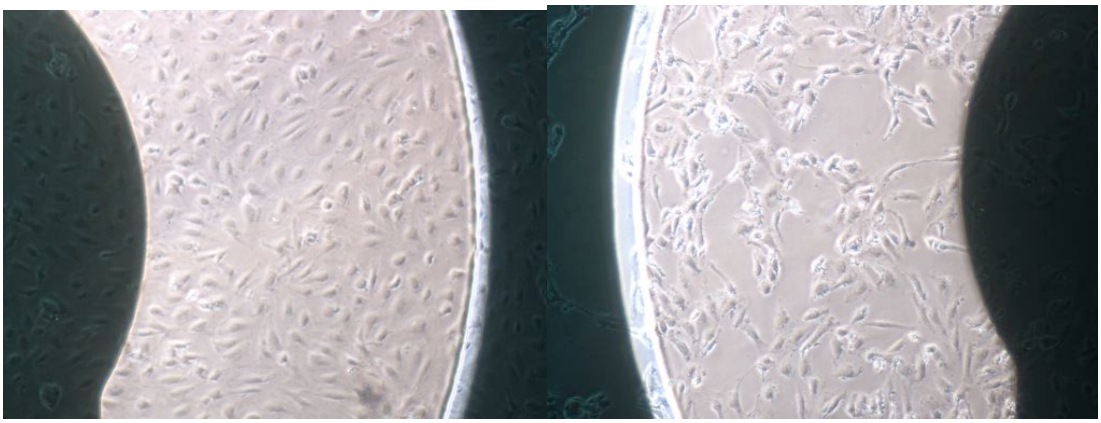

OPN vs uncoated condition adherent cells. Cells were stained for actin and nucleus (see adhesion assay protocol above)